UNIVERSIDAD
NACIONAL
DE COLOMBIA

Risk-based Resource Allocation for Management and Pandemic Response:

The COVID-19 Case in Bogotá, Colombia

Jeisson Andres Prieto Velandia
Computing and Systems Engineer

Universidad Nacional de Colombia
Facultad de Ciencias
Departamento de Matemáticas
Bogotá, D.C., Colombia
2020

Risk-based Resource Allocation for Management and Pandemic Response:

The COVID-19 Case in Bogotá, Colombia

Jeisson Andres Prieto Velandia
Computing and Systems Engineer

Thesis Presented to Obtain the Title of
M.Sc. in Applied Mathematics

Advisor
Jonatan Gómez Perdomo, Ph.D.

Research line
Risk-based Optimization

Research group
on Artificial Life ALIFE

Universidad Nacional de Colombia
Facultad de Ciencias
Departamento de Matemáticas
Bogotá, D.C., Colombia
2020

Title:
Risk-based Resource Allocation for Management and Pandemic Response: The COVID-19 Case in Bogotá, Colombia

Título:
Asignación de Recursos basada en Riesgo para la Gestión y Respuesta ante una Pandemia: El Caso del COVID-19 en Bogotá, Colombia

Abstract:
In any serious disaster, a gap develops between resource needs and resource availability. In a severe pandemic, this gap will be worse due to global supply chain disruptions or delays and the fact that governments and aid organizations will be overwhelmed responding to all who need assistance. Then, determining the locations of the resources (i.e., budget for antivirals and preventive vaccinations, Intensive Care Unit (ICU), ventilators, non-intensive Care Unit (non-ICU), doctors) to be used during a pandemic is a strategic decision that directly affects the success of pandemic response operations. The resource allocation could be done using a risk management perspective, where a demand point has one (or more) associated risk (i.e., geographic spread, overall poverty, medical preconditions) and the objective is to choose the amount to be invested in several interventions such that the overall risk exposed by the demand points is minimized according to budget constraints and health benefits. Due to the randomness and uncertainty of conditions, not only one but a set of risks may adversely affect the allocation of resources in the geographical space. Then, the objectives (one objective for each risk exposed) must be optimized simultaneously. However, there exists a trade-off among objectives, i.e., an improvement gained for one objective is only achieved by making concessions to another objective. This thesis aims to build a mathematically and computational grounded solution to the Multi-objective risk-based Resource Allocation problem suitable to be used for supporting decision making in the formulation of management and response policies during a pandemic. The risk management is studied in a complex network located in some space (city or town being studied). The risk in some specific place (demand point) is modeled not only by the vulnerability factor related to the severity of infection but also by the infectious disease transmission dynamics that emerged from the local interactions between people. The solution is framed in the current COVID-19 pandemic in Bogotá, the largest and most crowded city in Colombia.

Resumen:
En cualquier desastre grave, se desarrolla una brecha entre la necesidad y la disponibilidad de recursos. En una pandemia, esta brecha se agravará debido a las interrupciones o retrasos de la cadena de suministro global y al hecho de que los gobiernos y las organizaciones de ayuda se ven abrumados para responder a todos los que necesitan

asistencia. Entonces, determinar la ubicación de los recursos (por ejemplo, presupuesto para antivirales y vacunas preventivas, Unidad de Cuidados Intensivos (UCI), ventiladores, Unidad de Cuidados No Intensivos (no UCI), médicos) que se utilizarán durante una pandemia es una decisión estratégica que afecta directamente el éxito de las operaciones de respuesta ante una pandemia. La asignación de recursos se puede realizar utilizando una perspectiva de gestión de riesgos, donde un lugar de demanda tiene uno (o más) riesgos asociados (por ejemplo, propagación del virus, pobreza, precondiciones médicas) y el objetivo es escoger la cantidad que se invertirá en varias intervenciones tal que el riesgo expuesto por los puntos de demanda se minimiza de acuerdo con las limitaciones presupuestarias y los beneficios para la salud. Debido a la aleatoriedad y a la incertidumbre de las condiciones, no solo uno, sino un conjunto de riesgos pueden afectar negativamente la asignación de recursos en el espacio geográfico. Entonces, los objetivos (un objetivo por cada riesgo expuesto) deben optimizarse simultáneamente. Sin embargo, existe una compensación entre los objetivos, es decir, una mejora obtenida para un objetivo solo se logra haciendo concesiones en otro objetivo. Esta tesis tiene como proposito construir una solución con base matemática y computacional para el problema de la asignación de recursos basado en múltiples riesgos adecuada para apoyar a la toma de decisiones en la formulación de políticas de gestión y respuesta a pandemias. La gestión de riesgo es estudiada en una red compleja ubicada en algún espacio (ciudad o pueblo en estudio). El riesgo en algún lugar específico (punto de demanda) se modela no solo por factores de vulnerabilidad relacionados con la gravedad de la infección, sino también por las dinámicas de transmisión de la enfermedad que surgen por la interacción entre personas. La solución se enmarca en la actual pandemia de COVID-19 en Bogotá, la ciudad más grande y densamente poblada de Colombia.

Keywords:
Risk management, Risk-based optimization, Resource allocation, Pandemic response, Multi-objective optimization, Complex systems, COVID-19, Urban spatial analysis.

Palabras claves:
Gestión del riesgo, Optimización basada en riesgos, Asignación de recursos, Respuesta a pandemias, Optimización multiobjetivo, Sistemas complejos, COVID-19, Análisis espacial urbano.

Acknowledgements

This thesis becomes a reality with the kind support and help of many people. I would like to extend my sincere thanks to all of them.

Foremost, I want to express my gratitude towards my **family** (Cesar, Rosario, Julian, and Leydi) for the encouragement which helped me in the completion of this thesis. My beloved, **Vanessa** who is always by my side during the times I needed her most and helped me a lot in making this study.

I would like to express my special gratitude and thanks to my advisor, **Dr Jonatan Gómez** for imparting his knowledge and expertise in this study.

Dr. Elizabeth León and **Dr. Rafael Malagón**, for their collaboration and support.

My friend **Dr. Juan Jose Castro**, for sharing his knowledge and technical know-how.

My dissertation **Committee members** for taking some minutes of their valuable time to read this work and for their valuable suggestions.

This project would not have been possible without the funding, support and collaboration of the **Universidad Nacional de Colombia**, and especially, thanks to the Artificial Life (**ALIFE**) research group.

And to all those people who in one way or another, collaborated in the realization of this project, I extend my sincere gratitude.

Contents

Contents II

List of Tables IV

List of Figures V

Introduction VII

1. Theoretical background 1

1.1 Risk management 1

1.2 Complex Systems 3

1.3 Resource Allocation 5

1.4 Study Area and Data Sources 6

2. Modeling transmission dynamics for infectious diseases 8

2.1 Introduction 8

2.2 INFEKTA Agent-Based Model 9

2.3 Modeling Transmission Dynamics of COVID-19 in Bogotá 13

2.4 Summary 20

3. Vulnerability assessment for pandemics surveillance 22

3.1 Introduction 22

3.2 Urban Vulnerability Assessment 23

3.3 Vulnerability index for COVID-19 in Bogotá 27

3.4 Summary 33

4. Risk-based Resource Allocation for pandemic **35**

4.1 Introduction 35

4.2 Risk-based Resource Allocation 37

4.3 Resource allocation for COVID-19 in Bogotá 40

4.4 Summary 46

Conclusions and Future work **50**

Bibliography **53**

Appendix A: Supplementary Material **63**

Appendix B: Matrix Notation of RRA **64**

List of Tables

2.1 Data used in the simulation of INFEKTA 14

2.2 Number of interest places generated by *UPZ* group by *District* 15

2.3 Demographic information of virtual people grouped by *District* 16

2.4 Parameters of INFEKTA and their estimations for COVID-19 17

3.1 Summary of studies considered to vulnerability factors related with pandemics 26

3.2 Vulnerability domains for the COVID-19 case in Bogotá, Colombia 29

4.1 Statistics Δ_p and CPF metric values of the Pareto-optimal solutions 45

List of Figures

1.1 Spatial distribution of Bogotá using Zonal Planning Units (UPZ) and Urban sectors 6

2.1 General transmission dynamics of any infectious disease at individual level in INFEKTA 12

2.2 Example of 1000 georeferenced places in Bogotá and it's corresponding representation in the euclidean complex network 16

2.3 Example routines carried by individuals 18

2.4 Evolution of the epidemic dynamics 19

2.5 Sensitive analysis for the infection probability α 19

2.6 Social Distancing initialized at day 15 and ended at day 60 of the simulation 20

2.7 Comparison between total Seriously-Infected cases in INFEKTA and the real COVID-19 cases confirmed in Bogotá 21

3.1 Schematic diagram of the Urban Vulnerability Assessment for Pandemic Surveillance 24

3.2 Normalization for vulnerability factors using the probability integral transform 31

3.3 Vulnerability Ranking I with $k = 3$, index II with $k = 5$, and index III with $k = 10$ 32

3.4 Vulnerability indices generated using UVA for the current COVID-19 pandemic in Bogotá 33

3.5 Comparison between the vulnerability indices proposed and the real COVID-19 cases confirmed in Bogotá. 34

4.1 Configurations of the Risk-based Resource Allocation problem (RRA) 39

4.2 Complex network representation of Bogotá in the three RRA configurations 40

4.3 Risk indices generated for the current COVID-19 pandemic in Bogota 42

4.4 The approximate Pareto optimal solutions obtained 46
4.5 Solution visualized in the Bogotá using equal pseudo-weights 47
4.6 Solutions found with MoRRA over the real COVID-19 cases confirmed in Bogotá 49

Introduction

Motivation

Pandemics are large-scale outbreaks of infectious diseases that can greatly increase morbidity and mortality over a wide geographic area and cause significant economic, social, and political disruptions [65]. Significant policy attention has focused on the need to identify and limit emerging outbreaks that might lead to pandemics and to expand and sustain investment to build preparedness and health capacity [60]. The international community has made progress toward preparing for and mitigating the impacts of pandemics. The 2003 severe acute respiratory syndrome (SARS) pandemic and growing concerns about the threat posed by avian influenza led the World Health Assembly to update the International Health Regulations (IHR) to compel all World Health Organization member states to meet specific standards for detecting, reporting on and responding to outbreaks [82, 49]. Despite the great advances in the prevention and treatment of infectious diseases, the world is unaware to respond to a pandemic or any similarly global public-health emergency [83, 65].

Furthermore, the coronavirus COVID-19 pandemic has taught us that all efforts we made for prevention and treatment are not enough and that we are facing the global health crisis of our time. Since its emergence in Asia late last year, the virus has spread to every continent except Antarctica. Cases are rising daily in Africa, the Americas, and Europe [87]. As a result, increasing pressure has been placed on government agencies to do more with less, while also providing the necessary resources to respond efficiently and effectively during an emergency. However, government agencies have finite resources, so they can't monitor everything all of the time: they have to decide how best to allocate their scarce health resources (i.e., budget for antivirals and preventive vaccinations, Intensive Care Unit (ICU), ventilators, non-Intensive Care Unit (non-ICU), doctors) across a broad range of risk exposures during a pandemic [66, 4, 14]. This is called Risk-based resource allocation [31].

In the Risk-based resource allocation for a pandemic response, a demand point has one (or more) associated risk (i.e., geographic spread, routes of transmission, risk fac-

tors for infection, overall poverty, medical preconditions [127, 80, 65, 81]) and the objective is to choose the amount to be invested in several interventions such that the overall risk exposed by the demand points is minimized according to budget constraints and health benefits. Due to the randomness and uncertainty of conditions, not only one but a set of risks may adversely affect the allocation of resources in the geographical space. Then, the objectives (one objective for each risk exposed) must be optimized simultaneously [128, 113], but there exists a trade-off among objectives, i.e., an improvement gained for one objective is only achieved by making concessions to another objective.

Goals and Contribution

In line with the considerations mentioned above, this thesis aims to build a mathematically and computational grounded solution to the Risk-based Resource Allocation problem suitable to be used for supporting decision-making in the formulation of management and response policies during a pandemic. The solution is framed in the current COVID-19 pandemic in Bogotá, the largest and most crowded city in Colombia. This thesis aims to achieve the following goals:

- **Develop a Transmission Disease Model:** To understand the risk caused by the transmissibility of the disease, an Agent-Based Model (ABM) with transition disease dynamics will be proposed. The ABM will study the dynamics that emerged from the interaction between individuals in geographic space (city or town being studied).
- **Develop a Vulnerability Assessment Framework:** The risk in some specific place (demand point) is directly related to the vulnerability. A vulnerability assessment framework will be proposed in order to analyze not only the transmission dynamics that emerged by the ABM but also a set of vulnerability factors related to the severity of the infection.
- **Define the Risk-based Allocation Framework:** for management and pandemic response, a risk-based resource allocation framework is proposed. The model seeks to find an optimal allocation of a fixed amount of resources to geographical space such that risk(s) exposed by the demand point is minimized according to budget constraints and health benefits.
- **Test the model in a real-world scenario:** The transmission disease model, the vulnerability assessment framework, and the multi-risk-based resource allocation framework will be framed in the current COVID-19 pandemic in Bogotá, Colombia.

The main contribution of this work is to develop a new strategy to resource allocation in pandemics based on risk management methodologies. The following is a list of this thesis' contributions:

An Agent-based Model for Transmission of Infectious Diseases

In this work, an Agent-based Model (ABM) is introduced, called INFEKTA (Esperanto word for infectious), for modeling the transmission of an infectious disease. INFEKTA combines the transmission dynamics of an infectious disease with agents (individuals) that can move on a complex network of accessible places defined over a Euclidean space representing a real town or city. The applicability of INFEKTA is shown by modeling the transmission dynamics of the COVID-19 in Bogotá, Colombia. This work was published in *PLoS one* as a research article titled *INFEKTA—An agent-based model for transmission of infectious diseases: The COVID-19 case in Bogotá, Colombia* [39].

An Urban Vulnerability Assessment for pandemics

In this work, an Urban Vulnerability Assessment (UVA) methodology is proposed. UVA investigates various vulnerability factors related to pandemics to assess the vulnerability in urban areas. A vulnerability index is constructed by the aggregation of multiple vulnerability factors computed on each urban area (i.e., urban density, poverty index, informal labor, transmission routes). The applicability of UVA is shown by the identification of high vulnerable areas based on publicly available data where surveillance should be prioritized in the COVID-19 pandemic in Bogotá, Colombia. This work was published in *Sustainability* as a research article titled *Urban Vulnerability Assessment for Pandemic Surveillance: The COVID-19 case in Bogotá, Colombia* [86].

A Risk-based Resource Allocation Framework for pandemic preparedness

This work establishes a comprehensive risk-based emergency management framework that could be used by decision-makers to determine how best to manage medical resources, as well as suggest patient allocation among hospitals and alternative healthcare facilities. A set of risk indices are proposed by modeling the randomness and uncertainty of allocating resources in a pandemic. The city understudy is modeled as a Euclidean complex network, where depending on the neighborhood influence of allocating a resource in a demand point (i.e., informing citizens, limited social contact, allocation of a new hospital) different network configurations are proposed. Finally, a multi-objective risk-based resource allocation (MoRRA) framework is proposed to optimize the allocation of resources in pandemics. The applicability of the framework is shown by the identification of high-risk areas where to prioritize the resource allocation during the current COVID-19 pandemic in Bogotá, Colombia. This work was submitted for publication to *International Journal of Health Policy and Management* as a research article titled *Multi-objective Risk-based Resource Allocation for Urban Pandemic Preparedness: The COVID-19 Case in Bogotá, Colombia* [84].

Dissertation Outline

The remainder of this work is organized as follows:

Chapter 1 provides an augmented description of the background about the risk-based resource allocation problem, and the basic concepts applied in the development of the thesis.

Chapter 2 introduces an Agent-Based Model (ABM), called INFEKTA (Esperanto word for infectious), for modeling the transmission of infectious diseases.

Chapter 3 presents a vulnerability assessment framework for the quantification of the pandemic potential (severity of infection and transmissibility) which helps to prioritize surveillance to control highly vulnerable urban areas.

Chapter 4 establishes a comprehensive risk-based emergency management framework that could be used by decision-makers to determine how best to manage medical resources.

Finally, some conclusions and future research are outlined.

CHAPTER 1

Theoretical background

Some concepts are key to propose a comprehensive risk-based emergency management framework to manage medical resources. First, the risk management definition in this thesis is presented. Then, the complex system background is defined in order to understand the behavior of biological systems and their components. After that, some concepts of the resource allocation and multi-objective optimization problem are introduced. Finally, the study area and data sources used in this work are explained.

1.1 Risk management

What is a disaster

Schulz [100] defines disaster and Disaster Management (DM) as follows.

Definition 1.1.1. A **disaster** is an occurrence of widespread severe damage, injury, loss of life or property with which a community cannot cope and during which the society undergoes severe disruption.

Definition 1.1.2. Disaster Management (DM) is the range of activities designed to maintain control over disasters and emergencies and to provide a framework for helping at-risk persons to avoid or recover from the impact of the disaster.

The DM deals with situations before, during and after a disaster and the activities in the DM context are generally considered in four phases: *mitigation*, *preparedness*, *response*, and *recovery* [66, 4, 14]. Coppola [14] defines these phases as follows.

Definition 1.1.3. Mitigation involves reducing or eliminating the likelihood or the consequences of a hazard or both. Mitigation seeks to treat the hazard such that it impacts society to a lesser degree.

Definition 1.1.4. Preparadness involves equipping people who may be impacted by a disaster or who may be able to help those impacted with the tools to increase their chance of survival and to minimize their financial and other losses.

Definition 1.1.5. Response involves taking action to reduce or eliminate the impact of disasters that have occurred or is currently occurring, to prevent further suffering, financial loss, or a combination of both.

Definition 1.1.6. Recovery involves returning victims' lives to abnormal states following the impact of disastrous consequences. The recovery phase generally begins after the immediate response had ended and can persist for months or years thereafter.

The activities related to mitigation and preparedness, i.e.,pre-disaster phase, are considered as *Risk Management* while the activities related to response and recovery, i.e., post-disaster phase, are considered as *Crisis Management*.

Definition of Risk

Although there are different definitions of risk, this study uses the one given by [50]. Risk is composed by two components, *hazard*, and *vulnerability*.

Definition 1.1.7. Hazard is the probability that a disaster (i.e., COVID-19) occurs.

Definition 1.1.8. Vulnerability is the possibility that damages (i.e., fatalities, injuries, property damage, or other consequences) occur at a demand point because a resource is not allocated.

Risk is then defined as the expected damages due to a particular hazard for a given area and reference period. Based on mathematical calculations, the risk of the demand point i can be determined as a product of hazard (H) and vulnerability (V) [25].

$$R(i) = H(i) \times V(i) \tag{1.1}$$

Risk-based resource-allocation

There are four steps in a risk-based resource-allocation process [31]:

1. **Defining the risk:** The process begins by defining what risks the government agency cares about. Gaining a deep, clear, and common understanding of the risk exposures the government agency is tasked with addressing.
2. **Measuring the exposure:** Estimating the level of risk posed by specific targets is a critical input for prioritizing the deployment of constrained resources. First,

identify an expansive set of possible drivers of risk. Second, get historical data to understand what risks were realized. Finally, conduct statistical analysis to determine which of the possible drivers predict adverse events.

3. **Setting the strategy:** Once the risks have been defined and measured, the government agency needs to decide on an optimal strategy to deal with those risks. The government agency should have a strategy to mitigate the risks by decreasing both the likelihood and severity of an adverse event.

4. **Executing and learning**: Conducting risk-management activities, such as inspections, getting feedback on what is working and what is not, and learning from that feedback. Most agencies operate in a complex and dynamic environment, where there are unlimited opportunities to improve and the risks change over time.

1.2 Complex Systems

The complex system model approach considers a system as a large number of entities (equally complex systems that have autonomous strategies and behaviors) that interact with each other in local and non-trivial ways [64, 67, 99]. This approach provides a conceptual structure (a multi-level complex network [117, 58]) that allows characterizing the interrelation and interaction between elements of a system and between the system and its environment [7, 36, 5].

Compartmental Model

A compartmental model tracks changes in compartments without specifying which individuals are involved [37] and typically reflects health states relevant for transmission (e.g., susceptible, exposed, infectious, and recovered). These kinds of models represent epidemics of communicable disease using a population-based, non-spatial approach. The conceptual framework for this approach is rooted in the general population model which divides a population into different population compartments [52]. Compartmentalization typically reflects health states relevant for transmission (e.g., susceptible, exposed, infectious, recovered), though more partitioning is possible according to age and/or other relevant host characteristics. Heterogeneous and temporal behavior is modeled through the incorporation of relevant time-dependent social mixing, community structures and seasonality, relevant for infectious disease dynamics [75, 98]. Process dynamics are captured in transition rates, representing the rate by which an average individual transitions between compartments.

Agent-Based Models for infectious disease

Agent-Based Models (ABMs) are a type of computer simulation for the creation, disappearance, and movement of a finite collection of interacting individuals or agents with unique attributes regarding spatial location, physiological traits, and/or social behavior [45, 119, 123]. ABMs work bottom-up, with population-level behavior emerging from the interactions between autonomous individuals and their environment [95, 123]. They allow the history of every individual to be tracked and network structures to be explicitly represented. In general, ABMs allow [56]:

- To introduce local interaction rules at the individual level, which closely coincide with physical and social interaction rules.
- To include behaviors that may be randomized at the observational level, but can be deterministic from a mathematical point of view.
- To incorporate a modular structure and to add information through new types of individuals or by modifying current rules.
- To observe system dynamics that could not be inferred from the examination of the rules of particular individuals.

Complex network

A complex network is a graph with non-trivial topological features, features that model real systems in biology, economics, computer science, applied mathematics, and epidemiology [63, 112, 55, 109, 54]

Definition 1.2.1. An **undirected graph** G is pair (V, E), where V is a finite set and E is a binary relation on V. The set V is called the **vertex set** of G, and its elements are called vertices (singular: vertex). The set E is called the **edge set** of G, and its elements are called edges. The edge set E consists of an edge is a set (u, v), where $u, v \in V$ and $u \neq v$.

Definition 1.2.2. An **adjacent vertex** of a vertex v in a graph G is a vertex that is connected to v by an edge.

Definition 1.2.3. The **neighborhood** of a vertex v ($N(v)$) in a graph G is the subgraph of G induced by all vertices adjacent to v.

Definition 1.2.4. Regardless the metric space under consideration (points, spatial units, binary strings, DNA strands) [85], the **neighborhood class** $\mathcal{N}$ is defined as the set of all neighborhoods in a graph G, i.e., $\mathcal{N} = \{N(v) | v \in V\}$.

1.3 Resource Allocation

The resource allocation problem seeks to find an optimal allocation of a fixed amount of resources to activities to minimize the cost incurred by the allocation [72, 48].

Given a finite set of resources $\mathcal{R} = \{(r_1, r_2, \ldots, r_a) | r_i \in \mathbb{R}^+\}$ whose total amount is equal to T, it is required to allocate it to a activities so that the objective value $f(\mathcal{R})$ is minimized, see equation 1.2. The objective value may be interpreted as the cost or loss, or the profit or reward, incurred by the resulting allocation [48].

$$\begin{aligned} \textbf{min } & f(\mathcal{R}) = \sum_{i=1}^{a} f_i(r_i) \\ \textbf{subject to } & \sum_{i=1}^{a} r_i = T \\ & r_i \geq 0, i = 1, 2, \ldots, a \end{aligned} \tag{1.2}$$

where r_i represents the amount of resource allocated to activity i and $f_i(r_i)$ is the cost incurred by allocating the resource r_i at the i-th activity. If the resource is divisible, r_i is a continuous variable that can take any non-negative value. If it represents persons, processors, or trucks, on the other hand, variable r_i becomes a discrete variable that takes non-negative integer values (*discrete resource allocation problem*).

Multi-objective optimization

The multi-objective optimization problem (MoP) can be mathematically defined as follows.

$$\begin{aligned} \textbf{min } & f(x) = (f_1(x), f_2(x), \ldots, f_m(x))^T \\ \textbf{subject to } & x \in \Omega \end{aligned} \tag{1.3}$$

where $x = (x_1, x_2, \ldots, x_n)^T$ is the n-dimensional decision variable vector from the decision space Ω; $f : \Omega \rightarrow \Theta \subseteq \mathbb{R}^m$ consists a set of the m objective functions that map x from n-dimensional decision space Ω to m-dimensional objective space Θ.

Definition 1.3.1. Given two decision vectors $x, y \in \Omega$, x is said to Pareto **dominate** y, denoted by $x \prec y$, iff $f_i(x) \leq f_i(y)$, for every $i \in \{1, 2, \ldots, m\}$, and $f_j(x) < f_j(y)$, for at least one index $j \in \{1, 2, \ldots, m\}$.

Definition 1.3.2. A decision vector $x^* \in \Omega$ is **Pareto optimal** iff there is no $x \in \Omega$ such that $x \prec x^*$.

Definition 1.3.3. The **Pareto set (PS)** is defined as

$$PS = \{x \in \Omega | x \text{ is Pareto Optimal}\} \tag{1.4}$$

Definition 1.3.4. The **Pareto Front (PF)** is defined as

$$PF = \{f(x) \in \mathbb{R}^m | x \in \text{ PS } \} \tag{1.5}$$

Since objectives in (1.3) conflicted with each other, no point in Ω simultaneously minimizes all the objectives. The best trade-offs among the objectives can be defined in terms of PF.

1.4 Study Area and Data Sources

The proposed framework here is framed in the current COVID-19 pandemic in Bogotá city, the largest and most crowded city in Colombia. Bogotá is a metropolitan city with $7.412.566$ inhabitants living in an area of 1630 km^2 (410 km^2 urban and 1220 km^2 rural), at an altitude of 2640 m, with an annual temperature ranging from 6 to 20 °C, and annual precipitation of over 840 mm. Bogotá has composed of 621 Urban Sectors (Urban Sector is a cartographic division created by the National Administrative Department of Statistics (DANE) [22]). Each Urban sector belongs to one of the 112 Zonal Planning Units (UPZ) [107], see Figure 1.1.

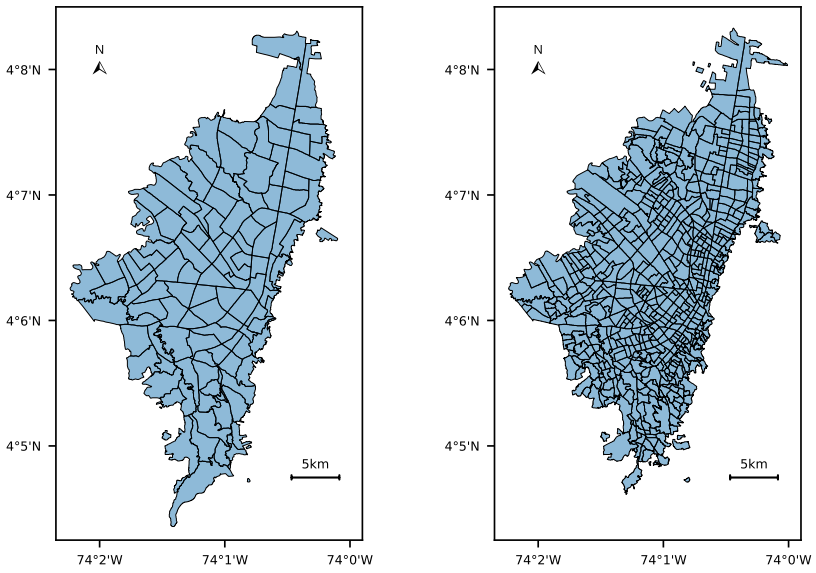

(A) Zonal Planning Units (UPZ) (B) Urban sectors

FIGURE 1.1. **Spatial distribution of Bogotá using Zonal Planning Units (UPZ) (left) and Urban sectors (right).**

The information used in this thesis is obtained from the National Department of Statistics (DANE), District Planning Secretary of Bogotá (SDP), and the District Mobil-

ity Secretary of Bogotá (SDM). Data comprised public information about demographic, transportation, socio-economic, and health conditions reported from 2011 to 2020. A summary of the datasets is presented as follows:

- MON_2017 [104, 106]: Dataset provided by SDP containing a set of monographs which provides a physical, demographic and socioeconomic description of Bogotá and its Zonal Planning Units (UPZ).
- SDM_2017 [103]: Dataset provided by SDM presenting detailed official information of mobility characterization in Bogotá.
- CNPV_2018 [22]: Dataset provided by DANE containing the national census made in 2018 which provides socio-demographic statistics of Colombia.
- DANE_2018 [23]: Dataset provided by DANE containing the results of the Multidimensional Poverty Index which encompasses educational and health quality, work and housing conditions, and access to public services.
- DANE_2020 [24]: Dataset provided by DANE presenting a vulnerability index based on demographic and health conditions relevant for COVID-19 pandemic.

Since the datasets' information are in different spatial units (i.e., Urban sectors, UPZ), the Urban sector is chosen for the study. Then, information at the UPZ level is transformed into Urban sectors by spatial transformation (i.e., UPZ values are assigned to each Urban sector contained in this).

CHAPTER 2

Modeling transmission dynamics for infectious diseases

This chapter presents an agent-based model, called INFEKTA, for simulating the transmission of infectious diseases, not only the COVID-19, under social distancing policies. INFEKTA combines the transmission dynamic of a specific disease, (according to parameters found in the literature) with demographic information (population density, age, and gender of individuals) of geopolitical regions of the real town or city under study. Agents (virtual persons) can move, according to its mobility routines and the enforced social distancing policy, on a complex network of accessible places defined over a Euclidean space representing the town or city. The transmission dynamics of the COVID-19 under different social distancing policies in Bogotá city, the capital of Colombia, is simulated using INFEKTA with one million virtual persons. A sensitivity analysis of the impact of social distancing policies indicates that it is possible to establish a 'medium' social distancing policy (i.e., close 40% of the places) to achieve a significant reduction in the disease transmission.

2.1 Introduction

Infectious diseases have a substantial impact on public health, health care, macroeconomics, and society. The availability of options to control and prevent the emergence, expansion, or resurgence of pathogens demands continuous evaluation using different methods. Mathematical models allow characterizing both the behavior and the emergent properties of biological systems, such as the transmission of infectious diseases. [61, 30, 5]. Many biological systems have been modeled in terms of complex systems since their collective behavior cannot be simply inferred from the understanding of their components [68, 70].

Computer-based algorithms are used to model properties and dynamic interactions between agents (e.g. persons, cells) or groups of agents within, and across levels of influence in complex systems [36, 58]. In general, agent-based modeling (ABM) can be used for testing theories about underlying interaction mechanics among the system's components and their resulting dynamics. It can be done by relaxing assumptions and/or altering the interaction mechanisms at the individual agent level. ABMs can increase the understanding of the mechanisms of complex dynamic systems, and the results of the simulations may be used for estimating future scenarios [56].

In the past, ABMs have been employed to address various infectious diseases such as, a bioterrorist introduction of smallpox [43], control of tuberculosis [78], implementation of distancing measures and antiviral prophylaxis to control H5N1 influenza A (bird flu) [33], design of vaccination strategies for influenza [13], devise evacuation strategies in the event of airborne contamination [29], and curtail transmission of measles through contact tracing and quarantine [28]. In the literature review, some other novel works that include heterogeneous agents and social distancing were proposed to model COVID-19 [32, 12].

In this chapter, an agent-based model approach is proposed, called INFEKTA (Esperanto word for infectious). INFEKTA mainly differs from existing works in that it aims to generate individuals and a complex network of places based on the population density of a determined city including individual interaction in public transportation means. INFEKTA models the disease transition at the person level and takes into consideration individual infection disease incubation periods and evolution, medical preconditions, age, daily routines (movements from house to destination places and back, including transportation if required), and enforced of Non-Pharmaceutical Interventions such as social distancing policies may flatten the curve.

The remaining of this chapter is organized as follows. Section 2.2 presents the agent-based model of infectious disease propagation, called INFEKTA, and its five-layer components. Section 2.3 describes the applicability of INFEKTA for modeling the transmission dynamics of the COVID-19 in Bogotá, Colombia. Finally, Section 2.4 discusses some of the conclusions and potential future developments.

2.2 INFEKTA Agent-Based Model

The agent-based model of infectious disease propagation, called INFEKTA, consists of five-layer components:

Space

The virtual space (for a city or town being studied) is a Euclidean complex network [117]: Nodes are places (located in some position of the 2D Euclidean space) where individuals can be at some simulation time and edges are routes (straight lines) connecting two neighbor places.

- **Place (Node)** - A place may be of three kinds: home (where individuals live), public transportation station (PTS), and interest place (IP) i.e., school, workplace, market, and transportation terminal. IPs and PTSs are defined in terms of capacity (maximum number of individuals that can be at some simulation step time). IPs and PTSs may be restricted, during some period, to some or all individuals. Place restriction is established according to the social distancing rule that is enforced during such a period.
- **Neighbor (Edge)** - A PTS is a neighbor to another according to the public transportation system of the city or town being studied. Homes and IPs are considered neighbors to its closest PTS in the 2D Euclidean space. No home is a neighbor to any other home neither an IP is a neighbor of any other IP. Finally, a home and an IP are considered neighbors if they are neighbors of the same PTS. Each individual has a Home and an IP. The closest distances are computed between each Home and IP and between these places with the closest PTS using their longitude and latitude. If the distance between a Home and IP is shorter than the distance to a PTS this home will be connected directly to an IP instead of their closest PTS. Otherwise, the closest PTS is connected to each Home and IP respectively. Detailed information can be found in Figure 2.2 of Section Virtual Space Setup.

Time

Virtual time is defined in INFEKTA at two resolution levels: days for modeling the transmission dynamics of the infectious disease, and hours for modeling the moving and interaction of individuals. Therefore, if an individual gets infected more than once during the same day, INFEKTA considers all of them as a single infection event. Any individual movement is carried on the same hour, it was started, regardless of the traveled Euclidean distance nor the length of the path (number of edges in the complex network).

Individuals

A virtual individual in INFEKTA is defined in terms of his/her demographic, mobility, and infectious disease state information.

- **Demographics** - The demographic information of a virtual individual consists of: **i) Age** of the individual; **ii) Gender** of the individual *female* o *male*; **iii) Location** of the individual at the current time step; **iv) Home** of the individual, **v) Impact level of medical preconditions** on the infectious disease state if the individual is infected, and **vi) IP interest** of going to certain type of IPs.

- **Mobility** - The ability of an individual to move through space (using the graph defining the space for determining the route as proposed in [92, 93]). Each individual has a **mobility plan for every day**, plan that is carried on according to the enforced social distancing policy and her/his infectious disease state. The mobility plan is modeled in INFEKTA as a collection of simple movement plans to have **i) Policy**: social distancing policy required for carrying on the mobility plan; **ii) Type**: may be *mandatory*, i.e., must go to the defined interest place) or *optional*, i.e., any place according to individual's preferences; **iii) Day**: day of the week the plan is carried on, maybe *weekly, weekend, Monday, ..., Sunday*; **iv) Going Hour** time an individual moves from Home to an IP; **v) Duration** in hours for coming back to home, and **vi) Place**: if the plan type is mandatory, it is a specific place, otherwise it is an IP selected by the individual according to his/her IP preferences.

Infectious Diseases Dynamic

Figure 2.1 shows the general transition dynamics of any infectious disease at the individual level in INFEKTA. This model can be adjusted to any specific infectious disease by setting some of the probabilities to specific values. For example, if no evidence recovered individuals become immune or susceptible again, such probabilities can be set to 0.0.

Any individual can potentially be in one of seven different infectious disease states or health states in INFEKTA: Immune (M), Susceptible (S), Exposed (E), Asymptomatic-Infected (I_A), Seriously-Infected (I_S), Critically-Infected (I_C), Recovered (R), Dead (D), and Immune (M). As it can be noticed, the terminology can be adapted from the compartmental models in epidemiology – namely, from the SEIR (Susceptible-Exposed-Infectious-Recovered) model. In INFEKTA, the infectious state of the SEIR model is divided into asymptomatic-infected, seriously-infected, and critically-infected in order to capture how age, gender, IP preferences, medical preconditions (co-morbidity), and social distancing policies can impact the evolution of the infectious disease in an individual. INFEKTA introduces both the M state since some individuals are naturally immune to or can become immune to (after recovering) certain infectious diseases and the Dead (D) state to distinguish between recovered and dead individuals.

Since rates are defined at the individual level, these rates can be defined by taking into consideration, for example, rates at the population level (obtained from a compartmental model), age, gender, and co-morbidity presented in the individual. Remem-

Infectious disease states
S := Susceptible
E := Exposed
I_A := Asymptomatic-Infected
I_S := Seriously-Infected
I_S := Critically-Infected
R := Recovered
M := Immune
D := Dead

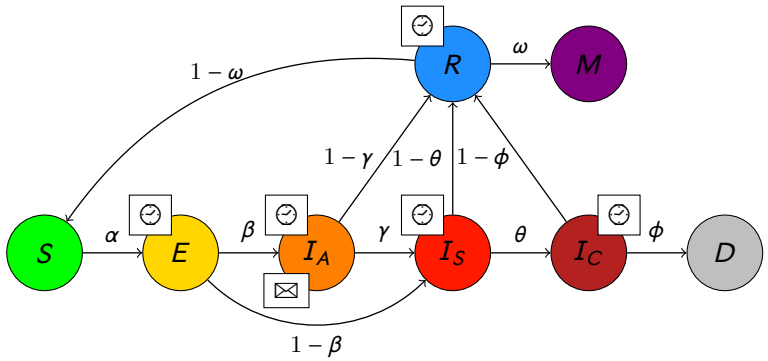

FIGURE 2.1. **General transmission dynamics of any infectious disease at individual level in INFEKTA.** Probabilities are individual based and are defined according to the infectious diseases and characteristic such as current location, age, gender, and so on. Symbol ⏲, on state X, indicates that an individual must stay some period of time $\mathcal{T}_X$ at such state X before being able to change to other state. Symbol ✉, indicates that individuals on state X can infect Susceptible (S) individuals.

ber that those rates are not defined at some time scale (as in compartmental models) but define the rule determining changes in the health status of individuals being close enough for interacting at the infectious disease transmission level or after some period of time being in some state. In this way, an individual can change with probability α from S state to state E if it are close enough to an asymptomatic-Infected (I_A) individual. Further, it will change from state I_A to state I_S with probability θ and if it has been on state I_A a period of time $\mathcal{T}_{I_A}$.

- α: is the transmission rate and incorporates the encounter rate between susceptible and infectious individuals together with the probability of transmission.
- β: is the rate at which individuals move from the Exposed (E) to the Asymptomatic-Infected state (I_S). It's complement ($1-\beta$) is the rate of individuals with symptomatic cases.
- γ: is the rate at which individuals move from the exposed (I_A) to the Seriously-Infected state (I_S).
- θ: is the rate at which individuals move from the Seriously-Infected (I_S) to the Critically-Infected state (I_C).
- ϕ: is the death rate.
- ω: is the immune rate that incorporates the probability of becoming immune.
- $\mathcal{T}_E$: Time an individual will be at the Exposed (E) state before changing to the Asymptomatic-Infected (I_A) or Seriously-Infected (I_S) states.
- $\mathcal{T}_{I_A}$: Time an individual will be at the Asymptomatic-Infected (I_A) state before changing to the Seriously-Infected (I_C) or Recovered (R) states.

- $\mathcal{T}_{I_S}$: Time an individual will be at the Seriously-Infected state (I_S) before changing to the Critically-Infected (I_C) or Recovered (R) states.
- $\mathcal{T}_{I_C}$: Time an individual will be at the Critically-Infected (I_C) before changing to the Dead (D) or Recovered (R) states.
- $\mathcal{T}_R$: Time an individual will be at the Recovered state (R) before changing to the Immune (M) or Susceptible (S) states.

INFEKTA can consider that two individuals are close enough for interacting at the transmission of the infectious disease if they are at the same place (home, interest place, or public transportation station) at the same time. To simplify this checking process, it is possible to consider that an individual just visited its home, final interest place, and both the initial and final PTSs when using the public transportation system.

Social Distancing Policy

The social distancing policy is described in INFEKTA as a finite sequence of rules, each rule having **i) Start Time**: an initial day for applying the social distancing policy rule; **ii) End Time**: final day for ending the social distancing policy rule; **iii) Level**: indicates the kind of restriction applied to the mobility of persons and accesses to places, and **iv) Enforce**: defines the specific mobility and access restrictions of the social distancing policy.

2.3 Modeling Transmission Dynamics of COVID-19 in Bogotá

INFEKTA is used for modeling the transmission dynamic of COVID-19 in Bogotá at level of UPZ[1]. Each *UPZ* belongs to one of the 19 urban *districts* in Bogotá. The urban perimeter population of Bogotá is $7.412.566$, and Bogotá massive public transportation system is called *Transmilenio* (**TM**). TM is a bus-based system, which has 143 stations and moves near to $2.500.000$ citizens every day.

Virtual Space Setup

Geographical information of Bogotá is used as the Euclidean space where the moving and interaction complex network is defined. Each one of the TM stations is located and added to the complex network according to the real TM system [110]. Also, the airport and the regional bus terminal are located and connected to the nearest TM station.

[1]Simplification is considered a fundamental part of modeling and simulation [118]. Although INFEKTA is model simplification of a real infectious disease dynamics, it is a model focused on system elements that matter, and that are feasible to understand.

Demographic information from 112 *UPZ* is used for generating in the Euclidean space interest places (Workplaces (W), markets (M), and schools (S)), homes (H), and people(P). Places are generated, in each one of the districts, following a 2D multivariate normal distribution $N \sim (\mu, \Sigma)$ (μ is the geographic center of the *UPZ* and Σ is the co-variance matrix defined by the points determining the perimeter of the district). The number of places in each *UPZ* is generated based on the population density of each UPZ according to the data available in 2017 [105]. Table 2.1 shows the amount of data generated for each type of place and people, also the number of TM stations (Bus), and terminal transportation that is used in the simulation, and Table 2.2 shows detailed information on the number of interest places generated by UPZ.

TABLE 2.1. **Data used in the simulation of INFEKTA.**

Agent	Instance	Type	Amount
Place	Home (H)	Home (H)	297260
	Public Transportation Station (PTS)	Bus (B)*	143
	Interest place (IP)	Workplace (W)	118952
		School (S)	59483
		Market (M)	98126
		Terminal (T)*	2
Individual	Individual	People (P)	998213

* Real places.

Figure 2.2 shows an example of 1000 virtual places in the Euclidean map of Bogotá [107]; also, the figure shows the associated complex network of connected places (nodes are places and edges are routed between places).

Individuals setup

An heterogeneous (varying gender, age, district and home) group of almost one million of individuals (998213) is generated using a stratified sampling based on the demographic information of the city for each district according to the projections to 2030 [105]. An individual is classified, according to her/his age, as: *Child* = [0-9], *Adolescent* = [10-19], *Adult* = [19-49], *Senior* = [50-69], and *Older* = 70+. Table 2.3 shows the total demographic information of virtual people.

The explicit impact level of medical preconditions on the state of the COVID-19 dynamic is not included in this preliminary modeling. The transition rates are wrapped in INFEKTA and allow modelers to change and play with different rates. Therefore, we set the initial values of these rates as shown in Table 2.4.

Also, a sequence of activities is randomly assigned to each individual to define a diary routine (in discrete intervals of 5 min). This is done according to the person's age and the hour of the day. For example, some agents *Adolescent* go to school, and some *Adult* agents go to work. Time to start a routine -going from Home to IP and return-

TABLE 2.2. **Number of interest places generated by *UPZ* group by *District***

	Amount of places			
DISTRICT	**Homes(H)**	**Markets(M)**	**Schools(S)**	**Workplaces(W)**
(01) Usaquén	19135	6307	3830	7625
(02) Chapinero	5410	1801	1100	2184
(03) Santa Fe	3944	1284	790	1578
(04) San Cristóbal	16806	5526	3367	6725
(05) Usme	14600	4840	2930	5875
(06) Tunjuelito	9106	2966	1817	3597
(07) Bosa	23103	7656	4650	9253
(08) Kennedy	40797	13452	8135	16322
(09) Fontibón	13458	4447	2688	5374
(10) Engativá	34428	11402	6906	13787
(11) Suba	41045	13517	8200	16423
(12) Barrios Unidos	9381	3101	1864	3776
(13) Teusaquillo	5896	1912	1163	2336
(14) Los Mártires	3921	1300	798	1581
(15) Antonio Nariño	4485	1503	885	1819
(16) Puente Aranda	10462	3454	2097	4189
(17) La Candelaria	1174	395	239	460
(18) Rafael Uribe	15282	5048	3058	6108
(19) Ciudad Bolívar	24827	8215	4966	9940
TOTAL	**297260**	**98126**	**59483**	**118952**

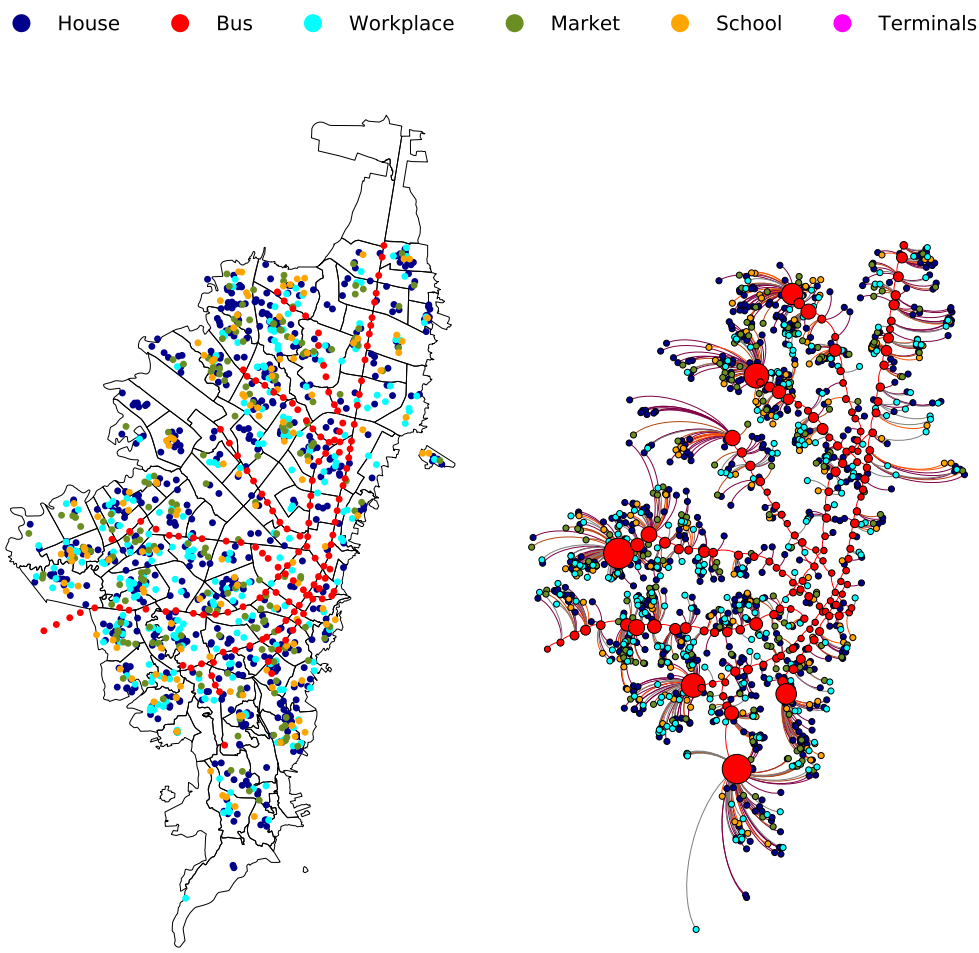

(A) Bogota with georeferenced places (B) Bogota complex network

FIGURE 2.2. **Example of 1000 georeferenced places in Bogotá (left) and it's corresponding representation in the euclidean complex network (right).**

TABLE 2.3. **Demographic information of virtual people grouped by *District*.** District (D), Total(T), Male(M), Female(F).

D	TOTAL			Child [0-9]			Adolescent [10-19]			Adult [19-49]			Senior [50-69]			older 70+		
	T	M	F	T	M	F	T	M	F	T	M	F	T	M	F	T	M	F
(01)	62358	33485	28873	11143	5601	5542	4599	2337	2262	28561	15163	13398	14157	7990	6167	3898	2394	1504
(02)	17459	9272	8187	2176	1075	1101	1199	598	601	8473	4410	4063	4148	2301	1847	1463	888	575
(03)	13145	6541	6604	2930	1371	1559	1076	509	567	5774	2856	2918	2554	1340	1214	811	465	346
(04)	51501	26341	25160	13343	6472	6871	4628	2269	2359	22840	11683	11157	8499	4625	3874	2191	1292	899
(05)	55236	27907	27329	16168	7801	8367	5378	2621	2757	24251	12321	11930	7940	4286	3654	1499	878	621
(06)	25394	12793	12601	5865	2791	3074	2228	1072	1156	11582	5815	5767	4340	2316	2024	1379	799	580
(07)	82103	41953	40150	22635	11015	11620	7200	3542	3658	37699	19349	18350	12313	6712	5601	2256	1335	921
(08)	135750	69517	66233	32179	15606	16573	10909	5349	5560	63480	32467	31013	24067	13080	10987	5115	3015	2100
(09)	48288	25416	22872	10311	5122	5189	3665	1840	1825	23352	12250	11102	8843	4923	3920	2117	1281	836
(10)	111026	57864	53162	22632	11102	11530	8331	4132	4199	52205	27028	25177	21980	12094	9886	5878	3508	2370
(11)	149078	78324	70754	33063	16409	16654	11747	5894	5853	70984	37201	33783	26900	14964	11936	6384	3856	2528
(12)	30578	15877	14701	5002	2418	2584	2052	1003	1049	13456	6867	6589	7579	4113	3466	2489	1476	1013
(13)	19180	10230	8950	2428	1205	1223	1283	642	641	8958	4680	4278	4812	2674	2138	1699	1029	670
(14)	12536	6210	6326	2365	1099	1266	947	445	502	5670	2776	2894	2742	1428	1314	812	462	350
(15)	13827	7090	6737	2999	1445	1554	1117	544	573	5968	3032	2936	2826	1528	1298	917	541	376
(16)	32801	16654	16147	6186	2948	3238	2474	1192	1282	15382	7731	7651	6563	3509	3054	2196	1274	922
(17)	3059	1434	1625	483	212	271	278	123	155	1369	633	736	731	360	371	198	106	92
(18)	47610	24149	23461	11532	5536	5996	4113	1995	2118	21440	10850	10590	8312	4471	3841	2213	1297	916
(19)	87284	44552	42732	25410	12375	13035	8172	4024	4148	38710	19868	18842	12614	6883	5731	2378	1402	976
TOTAL	**998213**	**515609**	**482604**	**228850**	**111603**	**117247**	**81396**	**40131**	**41265**	**460154**	**236980**	**223174**	**181920**	**99597**	**82323**	**45893**	**27298**	**18595**

TABLE 2.4. **Parameters of INFEKTA and their estimations for COVID-19.**

Symbol	Description	COVID-19 estimations					References
		Child	Teen	Adult	Senior	Older	
α	Probability of $S \rightarrow E$	0.180					[32]
β	Probability of $E \rightarrow I_A$	0.000	0.800		0.200		[16]
γ	Probability of $I_A \rightarrow I_S$	0.000	0.008	0.058	0.195	0.350	[121]
θ	Probability of $I_S \rightarrow I_C$	0.050	0.050	0.050	0.198	0.575	[32]
ϕ	Probability of $I_C \rightarrow D$	0.400		0.500			[32]
ω	Probability of $R \rightarrow M$	0.999					-
$\mathcal{T}_E$	Time (days) at E	$\Gamma(\alpha = 5.100, \beta = 0.860)$					[35]
$\mathcal{T}_{I_A}$	Time (days) at I_A	3	14		5		[9]
$\mathcal{T}_{I_S}$	Time (days) at I_S	$Triangular(7, 8, 9)$					[131]
$\mathcal{T}_{I_C}$	Time (days) at I_C	$Triangular(5, 7, 12)$					[131]
$\mathcal{T}_R$	Time (days) at R	$U(80, 100)$					-

is randomly selected in the interval from the 4h and 7h returning between the 17h and 20h. Some agents may move using the PTS and some others while going directly to their destination place. The route an individual takes is defined according to the complex network . Figure 2.3 shows three examples of different routines (paths over the graph) for the individuals.

Social Distancing Rule Setting

The level attribute of the social distancing rule for the COVID-19 in the virtual Bogotá is defined as follows:

- **None**: No restrictions to the mobility neither to access to places.
- **Medium**: Many places and few stations are restricted (depending on the type, capacity, etc). Some type of individuals is restricted to stay at home (except those with the required mobility level). i.e., close 40% of the places.
- **Extreme**: Few places are accessible to persons while few stations are restricted. Almost every individual is restricted to stay at home (except those with the required mobility level). i.e., close 80% of the places.

Results

The methodology of INFEKTA (Data preprocessing; places, population, and routes assignation; network creation) is available in a Github repository, see Appendix A. A total of 20 experiments are run and the results (COVID-19 dynamics, sensitive analysis, and social distance policies) shown below are the mean of those experiments. Figure 2.4 shows the evolution of the epidemic dynamics over time and for each *UPZ*.

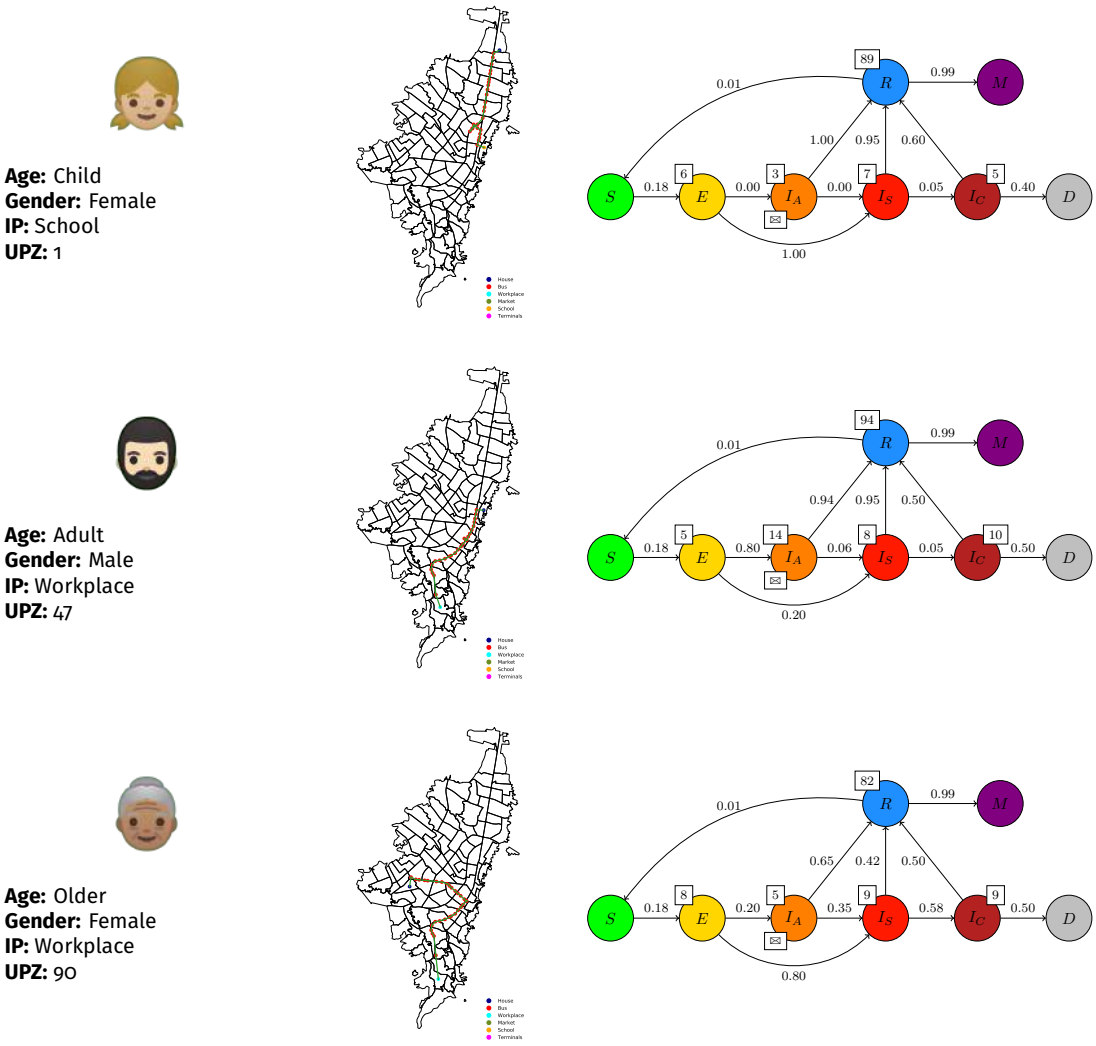

FIGURE 2.3. **Example routines carried by individuals.** Individual 38 (top): [Child, F, School, 1]; Individual 73128 (middle): [Adult, M, Workplace, 47]; Individual 349915 (bottom): [Older, F, Workplace, 90].

A sensitive analysis is made to the infection rate (α) parameter to check the robustness of the model. The sensitivity analysis is shown in Figure 2.5. Notice that by increasing or decreasing the infection disease rate (Figure 2.5 (left)), the peak of the transmission dynamics is reached sooner or later on time. When low infection disease rates, the number of cases is also low, reducing the impact on the economy. On the other hand, for high infection disease rates (Figure 2.5 (right)) the peak is reached in an early stage, and around half of the population is on one of the infected states (Asymptomatic, Seriously, Critically).

Also, different scenarios are analyzed, where each one of the social distancing policies is enforced just after 15 simulation days, see Figure 2.6. As it can be noticed, the evidence suggest how social distancing rules help to mitigate the exponential growth

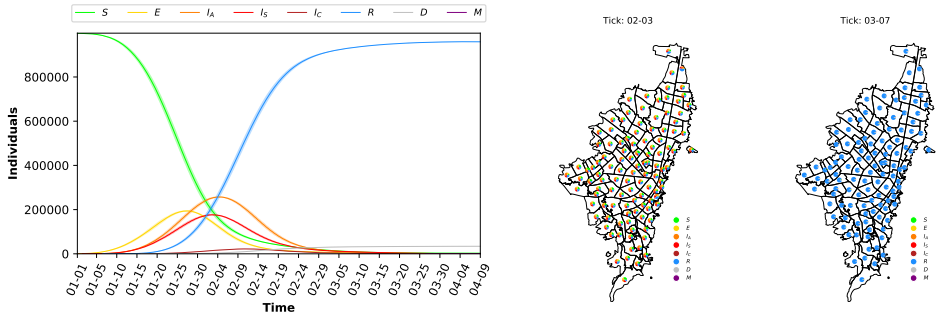

(A) Full dynamics over time (B) Dynamics for each UPZ at specific time

FIGURE 2.4. **Evolution of the epidemic dynamics.** Full dynamics over time (left), and dynamics for each *UPZ* at specific time (right).

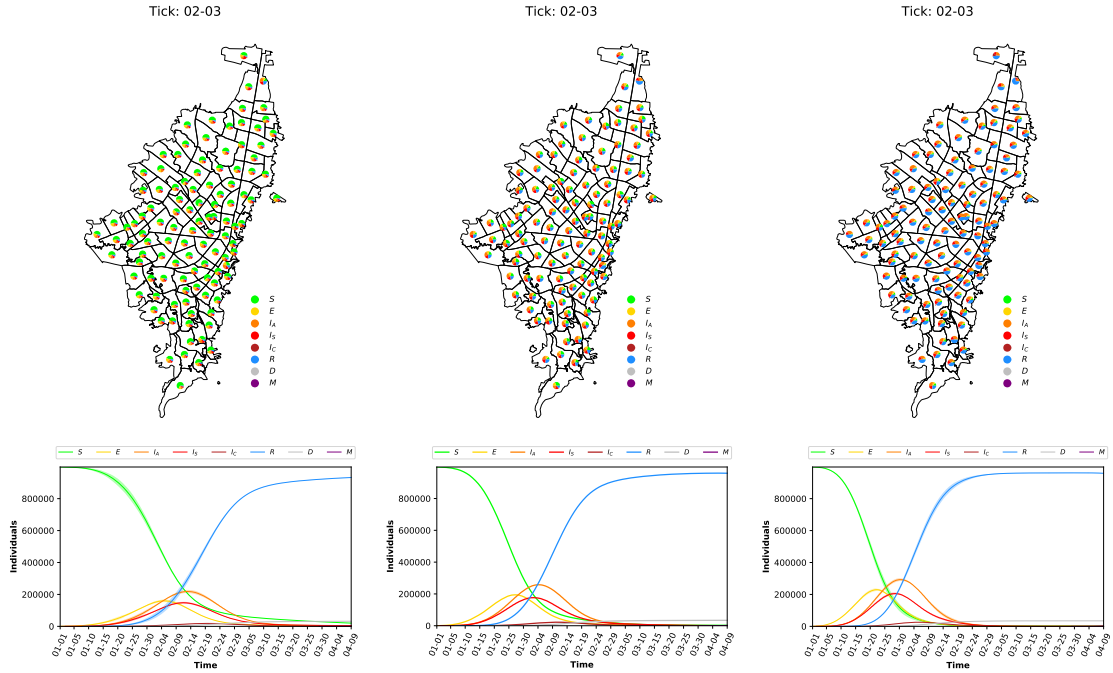

(A) $\alpha = 0.09$ (B) $\alpha = 0.18$ (C) $\alpha = 0.36$

FIGURE 2.5. **Sensitive analysis for the infection probability α.** $\alpha = 0.09$ (left), $\alpha = 0.18$ (middle), $\alpha = 0.36$ (right).

in the transmission disease dynamics (COVID-19), reducing the number of infectious cases (Asymptomatic, Seriously, and Critically). Interestingly, when the extreme social distancing rule (access to approximately 80% of interest places is restricted) the transmission disease dynamic displays a big second wave with more cases than the first wave.

Although the intention is not to predict geographic spread for the city, some similarities can be observed between the total Seriously-Infected cases in INFEKTA (we assume

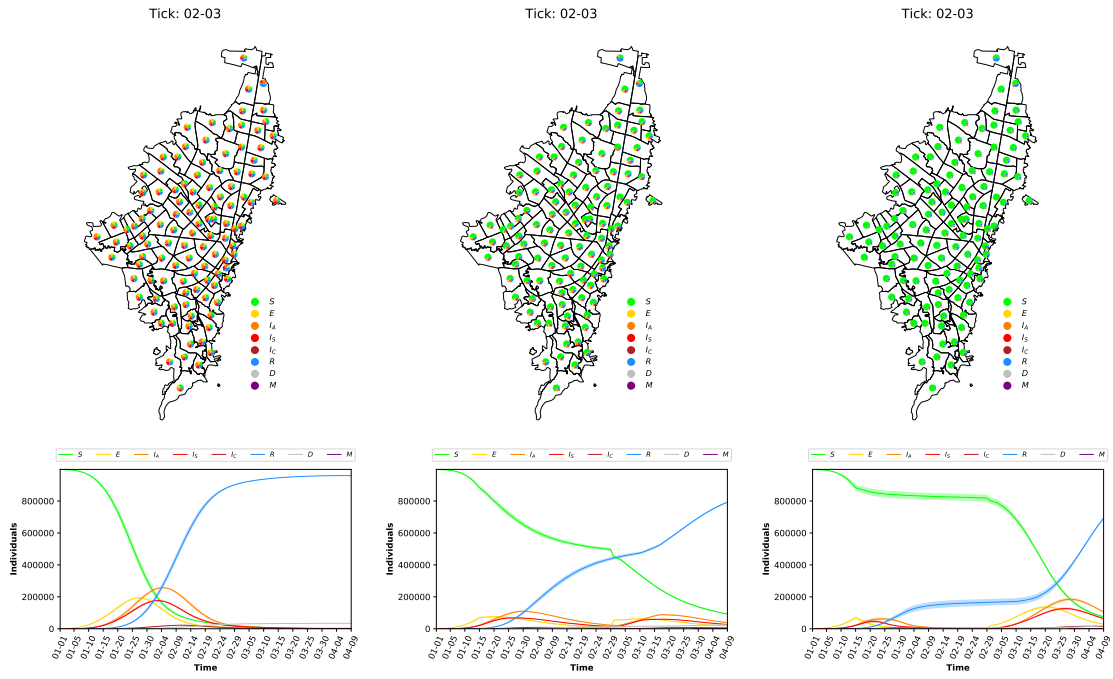

(A) None - No restrictions (B) Medium - close 40% of places (C) Extreme - close 80% of places

FIGURE 2.6. **Social Distancing initialized at day 15 and ended at day 60 of the simulation.** None - No restrictions (left), Medium - close 40% of places (middle), and Extreme - close 80% of places (right).

that individuals in Seriously-Infected state are cases tested in Bogotá) and the current concentration of COVID-19 cases confirmed in Bogotá [79], see Figure 2.7. The results show how UPZ with more cases found with INFEKTA matches with geographic areas with more COVID-19 cases. Then, how population distribution is generated from real density data of Bogotá, INFEKTA can be useful to explore policies by Zonal Planning Units (UPZ) or territorial divisions of a selected place providing to recommend actions for before, during, and after pandemic i.e., in planning and coordination efforts through leadership and coordination across sectors.

2.4 Summary

Modeling the Transmission dynamic of an infectious disease such as the COVID-19 is not an easy task due to its highly complex nature. When using an Agent-Based Model (ABM), several different characteristics can be modeled, for example, the demographic information of the population being studied, the set of places and the mobility of agents in the city or town under consideration, social distancing rules that may be enforced, and the special characteristics of the infectious disease being modeled. INFEKTA is an ABM that allows researchers to combine and study all of those characteristics.

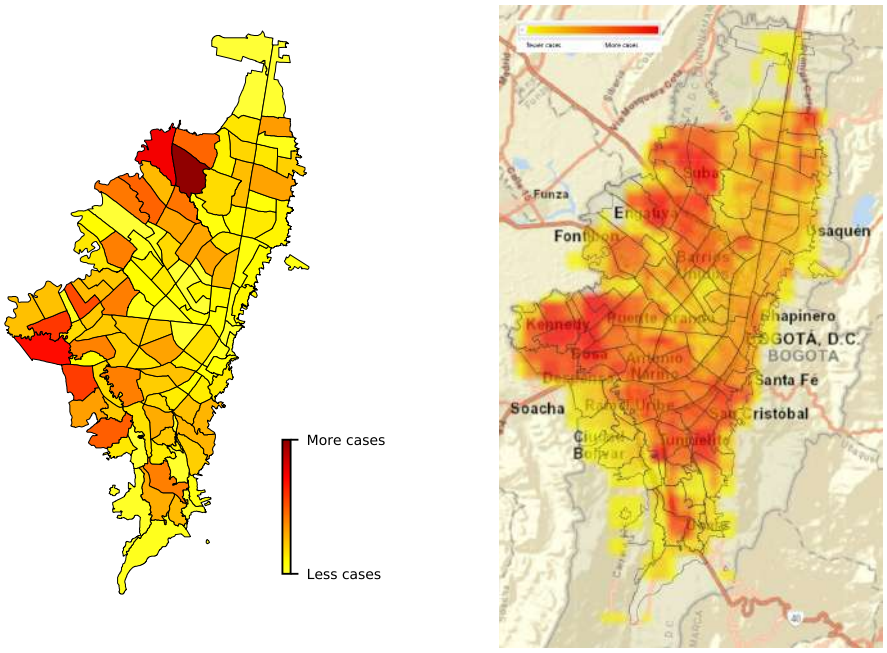

(A) Total Seriously-Infected cases in INFEKTA (B) Real COVID-19 cases confirmed in Bogotá

FIGURE 2.7. **Comparison between total Seriously-Infected cases in INFEKTA (left) and the real COVID-19 cases confirmed in Bogotá (right).** The colored boxes in the right map (confirmed cases map) corresponds to the concentrations of the cases in 1000 meters on December 30, 2020, in Bogotá.

The preliminary results modeling the transmission dynamics of the coronavirus COVID-19 in Bogotá city, the largest and most crowded city in Colombia, indicate that INFEKTA may be a valuable asset for researchers and public health decision-makers for exploring future scenarios when applying different social distancing policy rules and controlling the expansion of an infectious disease. Although this study is doing a rough and not so real approximation of the transmission dynamics of the COVID19, similar behaviors can be contained, in the preliminary experiments, to those reported for the COVID-19 in the real world. Therefore, INFEKTA may be able to provide more accurate results if its parameters are set to real ones: disease transmission rates, virus, incubation periods, comorbidity, houses, interest places, routines, population size (close to nine million virtual individuals for Bogotá).

The next chapter introduces a vulnerability assessment framework to analyze not only the transmission dynamics that emerged by the INFEKTA, but also a set of vulnerability factors related to infectious diseases.

CHAPTER 3

Vulnerability assessment for pandemics surveillance

In this chapter, an Urban Vulnerability Assessment (UVA) methodology is proposed. UVA investigates various vulnerability factors related to pandemics (severity of infection and transmissibility) to assess the vulnerability in urban areas. A vulnerability index is constructed by the aggregation of multiple vulnerability factors computed on each urban area (i.e., urban density, poverty index, informal labor, and transmission routes). This methodology is useful in a-priori evaluation and development of policies and programs aimed at reducing disaster risk (DRR) at different scales (i.e., addressing urban vulnerability at national, regional, and provincial scales), under diverse scenarios of resources scarcity (i.e., short and long-term actions), and for different audiences (i.e., the general public, policy-makers, international organizations). The applicability of UVA is shown by the identification of high vulnerable areas based on publicly available data where surveillance should be prioritized in the COVID-19 pandemic in Bogotá, Colombia.

3.1 Introduction

Vulnerability Assessment describes the degree to which socioeconomic systems and physical assets in geographic areas are either susceptible or resilient to the impact of a disaster (i.e., pandemic). Once the vulnerability is evaluated across areas, it is possible to prioritize them and undertake preventative action and response efforts (i.e., planning and coordination, reducing the spread of disease, and continuity of health care provision) [17, 73, 81, 65]. In the urban context, the Urban Vulnerability Assessment (UVA) helps to determine what types of preparedness and response activities might support an optimal Urban Strategic Planning (USP) to assist the decision-making processes [96].

Several models have been proposed to establish vulnerable urban areas over the infectious disease domain, that is, vector-borne diseases [42], Dengue [17], malaria [53, 41],

and Ebola [73]. Recently, in [69] a COVID-19 vulnerability index for urban areas in India was proposed which aggregates weighted scores of a set of variables related to COVID-19 precaution of social distance and lockdown in four metro cities in India. Nevertheless, relative preferences between criteria-based judgments for the gathering of preferences for indicators (vulnerability factors) is needed in those models, having some limitations such as expert bias, or hierarchical criteria to weight the factors [122, 76].

On the other hand, the recently UN-Habitat response plan for the current COVID-19 pandemic underlined the urban-centric character of the disease, indicating that above 95% of the cases are located in urban areas [116]. The World Health Organization (WHO) emphasized that the first transmission in the COVID-19 pandemic did happen in the internationally connected megacities [126]. Further, interconnected cities in South America (i.e., Bogotá) are presumably more susceptible given their population densities, low income, job informality, and lack of affordable health services [71].

In this chapter, a conceptual framework for Urban Vulnerability Assessment (UVA) for pandemics is proposed. This UVA conducted a comprehensive review of relevant literature to identify vulnerability factors influencing pandemics. These are then condensed into an index that allowed to establish and rank potentially vulnerable urban areas. The vulnerability rank is built using Borda's count aggregation method, which does not need experts knowledge nor additional parameters. UVA is framed in the current COVID-19 pandemic in Bogotá, the most densely populated city of Colombia. Using publicly available data of Bogotá, UVA creates a spatially explicit description of vulnerability for the COVID-19 pandemic. This modeling application study provides a potential tool to inform policy-makers to prioritize resource allocation and devise effective mitigation and reconstruction strategies for affected populations in Bogotá.

This chapter is divided into three sections. Section 3.2 develops the methodology of Urban Vulnerability Assessment (UVA) for pandemic surveillance. Section 3.3 describes the applicability of UVA for the current COVID-19 pandemic in Bogotá, Colombia. Finally, Section 3.4 discusses some of the conclusions and potential future developments.

3.2 Urban Vulnerability Assessment

The conceptual framework of Urban Vulnerability Assessment (UVA) for pandemics surveillance is illustrated in Figure 3.1. UVA involves four main stages. The first stage is the identification of vulnerability factors influencing pandemics (Figure 3.1, panel (a)). The second stage is to transform the raw input data from each vulnerability factor into a probability distribution (Figure 3.1, panel (b)). The third stage groups geographic areas with similar characteristics into classes to assign a vulnerability level (Figure 3.1, panel (c)). After that, an aggregation method is applied to create a unique rank for each class

(Figure 3.1, panel (d)), where a higher rank is assigned to a higher vulnerability level (Figure 3.1, panel (e)).

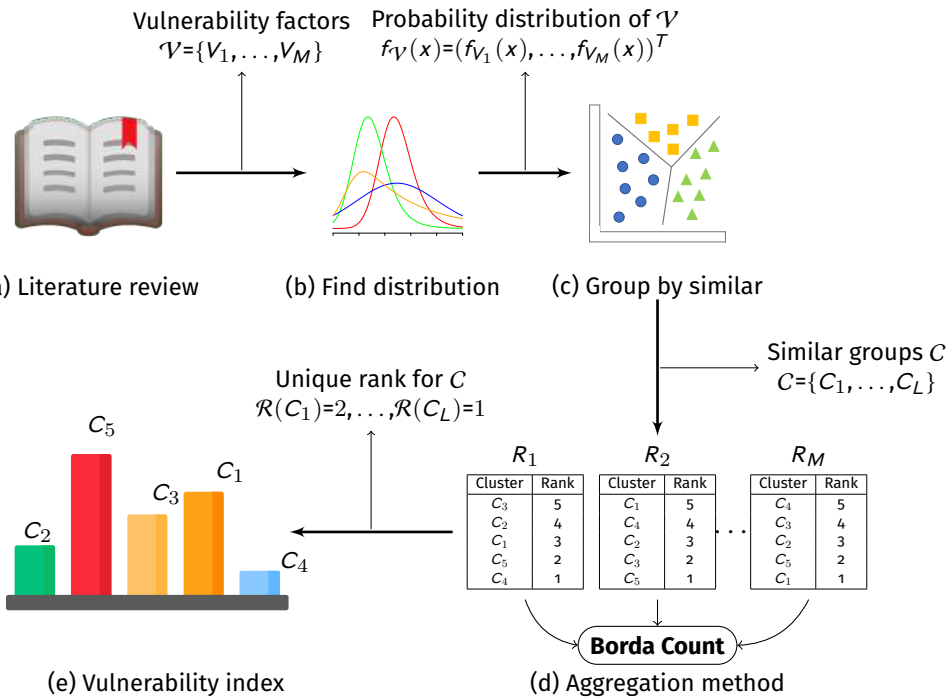

FIGURE 3.1. **Schematic diagram of the Urban Vulnerability Assessment for Pandemic Surveillance.**

Literature Review

A focused literature search [59] is conducted to identify a set of peer-reviewed studies that possibly examined types of vulnerability factors related to pandemics. The studies consider both factors related to past pandemics (i.e, 1881 Fifth cholera, 1918 Spanish flu influenza, 1957 Asian flu influenza, 2003 SARS, 2009 h1n1, 2013 West Africa Ebola) and factors found in the current COVID-19 pandemic. The literature search used a combination of search strings to retrieve studies in the Google Scholar database (i.e., (hazard OR uncertain* OR risk* OR vulnerab*) AND (disease OR pandemic* OR endemic*) AND (analysis OR factor* OR assess*)). The search included peer-reviewed English language journal articles (called “studies” in the review) published between 1982 and 2020. The retrieved studies for which the study’s title, abstract, or keywords indicated the study examined a type of vulnerability in pandemics. Then, a manual assessment is made for every study against eligibility criteria:

- The study provided a quantitative or conceptual analysis of vulnerability factors related to infectious diseases (or pandemics).
- The core of the study included vulnerability.

- The study focuses on urban areas.
- The study focuses more on the vulnerability at the geographic area level than on the individual level.

Afterward, the vulnerability factor the study focused on, the geographic focus of the study, and the methods used to assess the vulnerability are recorded. This involved examining the title, abstract, keywords, or full-text version. The country or region(s) where the study focused is listed. For theoretical studies without a clear geographic focus, the geographic location is listed as Not Applicable (NA). Table 3.1 summarizes the 11 studies that are considered for the analysis of vulnerability factors related to pandemics.

Statistical Data Analysis

Let $\mathcal{S}$ be a geographical space under investigation (i.e., state, country, or city) defined in terms of a finite set of P smaller spatial units (i.e. countries, census tracts, or zip codes); that is $\mathcal{S} = \{1, 2, \ldots, P\}$. Let $\mathcal{V}$ be a set of M vulnerability factors, and V_k the values of the P spatial units in the k-th vulnerable factor $V_k = \{v_{k,1}, \ldots, v_{k,P}\}$. The raw data for each factor are normalized across all spatial units over the range 0 (best) to 1 (worst). Different normalization methods exists in the literature [40]. The method chosen in this study is to build an estimation of the Probability Density Function (PDF) of the data, and then transform it via its Cumulative Density Function (CDF), so intervals with higher likelihood of containing data are assigned to higher portion of the normalized interval [0,1]. This is called probability integral transform [6]. An estimate to the PDF f_{V_k} at specific spatial unit x is made using the Kernel Density Estimation (KDE) method.

$$f_{V_k}(x) = \frac{1}{P\lambda} \sum_{i=1}^{P} \mathcal{K}_\lambda(x, v_{k,i}), \tag{3.1}$$

where $\mathcal{K}$ is the kernel (a non-negative function) and λ is the smoothing parameter called the bandwith.

Then, to normalize the raw data at spatial unit x over the range 0 (best) to 1 (worst) in the k-th vulnerable factor, the probability integral transform is applied.

$$x' = F_{V_k}(x), \tag{3.2}$$

where F_{V_k} is the CDF of the k-th vulnerable factor.

TABLE 3.1. **Summary of studies considered to vulnerability factors related with pandemics.**

Reference	Vulnerable Factor(s)	Geographic Focus	Methods	Main Findings
[10]	a. Essential worker b. Household size c. Age d. Gender	Singapur	Demographic, clinical, treatment, and laboratory data	Describe incidence and vulnerability factors for pandemic in healthcare personnel
[65]	e. Geographic spark f. Geographic spread g. Burden quantification h. Disease importation a. Essential worker i. Healthcare access	NA	Epidemiology evidence of previous infectious diseases	Covers the concerning of vulnerability, impacts, mitigation and pandemic knowledge gaps
[46]	j. Medical preconditions c. Age d. Gender a. Essential worker	United Kingdom	Epidemiology evidence of COVID-19	How the vulnerability might vary in different population groups or settings
[47]	k. Time delay illness l. Insufficient follow-up c. Age d. Gender	China	Demographic, clinical, treatment, and laboratory data	Provides insights in early vulnerability assessment using publicly available data
[80]	i. Hospital capacity m. Water and sanitation n. Logistics o. Per capita income p. Public education	NA	Conceptual framework for epidemic preparedness and response	Epidemic Preparedness Index (EPI) for assessing resilience to epidemic and pandemic outbreaks
[73]	i. Health infrastructure q. Urban density f. Disease dynamics r. Economic growth	NA	Literature review and expert elicitation	Identify the most vulnerable countries to infectious disease outbreaks
[74]	q. Urban density s. High-density facilities h. Worldwide movement m. Inadequate sanitation	NA	Epidemiology evidence of previous infectious diseases	Identification of specific factors responsible for disease emergence
[111]	o. Socioeconomic status c. Age t. Rural or urban living	New Zealand	Epidemiology evidence of previous infectious diseases	Description of vulnerability factors for death in an outbreak of pandemic
[81]	u. Public transportation s. Nearby food market o. Overall poverty rate i. Healthcare access v. Public services access	NA	Vulnerable indicators for area classification	Identify geographic areas to be prioritized for preventative action and response efforts
[127]	f. Geographic spread k. Infectious period	NA	Demographic, clinical, treatment, and laboratory data	Epidemiological modeling to reduce the disease burden
[1]	p. Education levels o. Poor households t. Urbanization q. Population density m. Housing condition i. Health care availability j. Chronic morbidity	India	Epidemiology evidence of COVID-19	Social vulnerability index for management and mitigation of COVID-19

Note: Studies retrieved from the literature search. NA means not applicable.

Cluster Analysis

To identify spatial units with similar levels of vulnerability, areas with similar vulnerability profiles are clustered. Here, the cluster analysis uses the information contained

in their vulnerability profile (expressed from their CDF for the M vulnerability factors) to form spatial groups that are relatively homogeneous in vulnerability, that is, synthesize the spatial units into k partitions.

UVA allows the decision-maker to select the number of cluster partitions in which the spatial units will be grouped (i.e., the selection made according to the number of vulnerability levels desired). Each sub-set of solutions $C = \{C_1, \ldots, C_L\}$ obtained by a cluster algorithm [3] (i.e., k-means) contains a number P_j of spatial units of similar characteristics. In this way, the decision tool makes it possible to obtain a suitable number of k relevant possible vulnerable assessments (i.e., $k = 3$ vulnerability of low, medium, and high; $k = 10$ vulnerability from 1 to 10).

Create Vulnerability Index

To assign a vulnerability level (rank) to each cluster, a Borda's count aggregation method is proposed [27]. The Borda's method takes as input a set of ranks $R = \{R_1, \ldots, R_M\}$ (where R_k is an order of the Clusters $C = \{C_1, \ldots, C_L\}$ in the k-th vulnerability factor), and produces a single rank by mixing the orders of all the input ranks. The number of points (weight) assigned for each ranking varies depending on which variant of the Borda count is used. For this, let $t_{R_k}^{C_i}$ be the position of the Cluster C_i in the rank R_k, and w_{R_k} the weight assigned for the rank R_k. A new aggregated value of ranking or the i-th Cluster is defined as:

$$\mathcal{R}(C_i) = \sum_{k=1}^{M} w_{R_k} \left(|C| - t_{R_k}^{C_i} \right). \tag{3.3}$$

To assign a vulnerability level, vulnerability factor ranks R_k are made by sorting the centroid values of C_i for each M vulnerability factor. Next, these M ranks ($R = \{R_1, \ldots, R_M\}$) are combined using Borda's count aggregation method to obtain a unique aggregated vulnerability rank.

Finally, the vulnerability rank is associated with a vulnerability index, that is, a higher rank indicates higher vulnerability.

3.3 Vulnerability index for COVID-19 in Bogotá

The methodology of UVA (Data preprocessing; normalization, cluster definition, and aggregation method; vulnerability indices) is available in a Github repository, see Appendix A.

Vulnerability Domains

Given the data of the Urban sectors of Bogotá and the vulnerability factors found in the literature review (see Section 3.2), a set of three relevant domains is proposed: (i) Where and how a person lives,(ii) Where and how a person works, and (iii) Where and how a person moves around (The proposed domains are used for the convenience of the reader and could change depending on the data analysis made in the geographic area. It helps the reader to associate vulnerability factors related. These domains do not influence the process of assigning vulnerability to a spatial unit.). These three domains contain the input for the quantitative analysis. Table 3.2 shows the domains proposed and the vulnerability factors associated with them.

- **Where and how a person lives:** Several demographic factors influence the degree of vulnerability of the urban sector to the pandemic. The literature emphasizes factors such as urban density, age, and the urban living (i.e., socio-spatial segregation). The level of education or literacy, and the quality of the health care system (i.e., included in the poverty index) can also play a helpful role in mitigating the spread and effects of infectious diseases [73]. Further, most data on the COVID-19 pandemic suggest that people with underlying comorbid conditions such as high blood pressure, diabetes, respiratory and cardiovascular disease, and cancer are more vulnerable than people without them.
- **Where and how a person works:** Urban sectors with high-density facilities (i.e, educational buildings, cultural buildings, sports buildings, food markets, all formal labor) are more vulnerable to the spread of contagious diseases due to space limitations within and between households, growth and mobility, and limited water, sanitation, and hygiene (WASH) infrastructure. Also, most workers in the informal economy (i.e., informal labor) have higher exposure to occupational health and safety vulnerability as they have no appropriate protective equipment, are forced to work daily for their sustenance, and must afford all their expenses from cash out-of-pocket due to their limited banking access [44].
- **Where and how a person moves around:** Understanding transmissibility, risk of geographic spread, transmission routes, and infection vulnerability factors (i.e., geographic impact) provides the baseline for epidemiological modeling that can inform the planning of response and containment efforts to reduce the burden of disease [127]. Also, there have been claims that the use of public transport (i.e., public transportation dependency) increases the likelihood of the disease spreading [81].

TABLE 3.2. **Vulnerability domains for the COVID-19 case in Bogotá, Colombia.**

Vulnerability Domains	Vulnerability Factor(s)	Definition	Dataset
Where and how a person lives	Urban density (q.)	Number of people inhabiting a given urban area	CNPV_2018
	Age (c.)	Number of people aged 15–34 years (SARS-CoV-2 incidence increased [38])	CNPV_2018
	Comorbidities (j.)	Groups areas according to their demographics and co-morbidities	DANE_2020
	Poverty index (p. and i.)	Multiple deficiencies in health, education and standard of living	DANE_2018
	Socio-spatial segregation (t.)	Absence of interaction between individuals of different social groups	[2] *
Where and how a person works	Educational (s.)	Number of educational buildings (i.e., preschool, primary and high-school, research centers, technical training centers, Universities)	MON_2017
	Cultural (s.)	Number of cultural buildings (i.e., theaters, concert halls, libraries, museums, civic centers, community halls)	MON_2017
	Sports (s.)	Number of sports buildings (i.e., stadiums, coliseums, sports clubs, country, racetracks, swimming pools)	MON_2017
	Food markets (s.)	Number of food market buildings (i.e., Central market, market square)	MON_2017
	Formal Labor (s.)	Number of commercial buildings with license	MON_2017
	Informal Labor (s.)	Percentage of informal employed according to its workplace	[108] *
Where and how a person moves around	Public Transportation Dependency (u.)	Number of Trips generated throughout the day (trips longer than 15 min)	SDM_2017
	Transmission routes (f.)	Asympthomatic number people at the peak of the pandemic	INFEKTA *
	Geographic impact (k.)	Number of dead people after 100 simulation days	INFEKTA *

Note: Letters in the table refer to factors presented in the Section 3.2, Table 3.1.
* Values calculated in the cited paper.

Vulnerability Analysis

To understand the distribution of the vulnerability factors over the urban sectors, the raw data for each factor is normalized across all urban sectors over the 0 (less vulner-

able) to 1 (most vulnerable) range. Figure 3.2 shows the normalization for the three domains. The vulnerability value for each factor is associated with the probability integral transform using the KDE method (KDE uses the Gaussian kernel for its estimations and Scott's Rule for the bandwidth selection [102].). The results show the spatial correlation that exists for some vulnerability factors, especially for the Where and how she/he works domain. In contrast to the Where and how she/he lives domain, the spatial correlation is not clear and the vulnerability is distributed across the geography area under study (Bogotá).

Vulnerability Index

To provide a better vulnerability characterization, the UVA framework generates three different indices to assess vulnerability in various ways (depending on the cluster partitions). Vulnerability index I has three different clusters that distinguish low, medium, high exposure groups to disease harm. Index II has five different clusters ($k = 5$) to distinguish lowest, low, medium, high, highest vulnerability groups. And, index III has ten clusters ($k = 10$) to represent vulnerability groups on a scale from 1 to 10. Figure 3.3 shows the cluster analysis made to build the vulnerability indices. The clusters' centroids (Figure 3.3-middle) are used to sort the vulnerability factors in descending order. This sort is interpreted as vulnerability ranking which is used for the analysis. Then, to aggregate the 14 ranks (one for each vulnerable factor in Table 3.2) in a unique vulnerability ranking the Borda's method is used (Figure 3.3-bottom). The unique vulnerability ranking is then transformed into a vulnerability index, where a higher rank indicates higher vulnerability. In absence of a rationale for using any weighting, scheme [91, 97, 69], equal weights are assigned to each vulnerable rank for calculating the overall vulnerability index, according to other studies [34, 1].

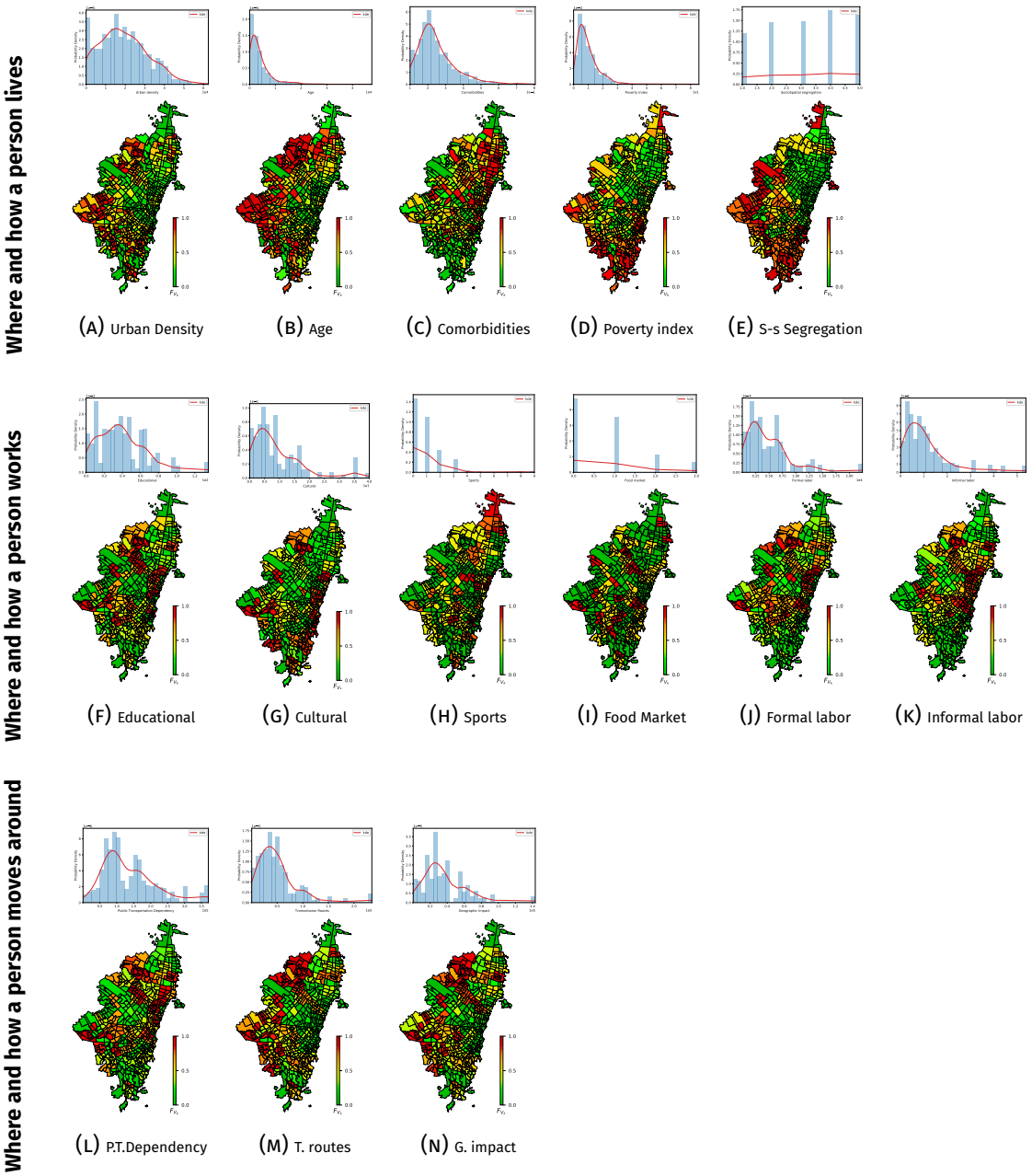

FIGURE 3.2. **Normalization for vulnerability factors using the probability integral transform.**

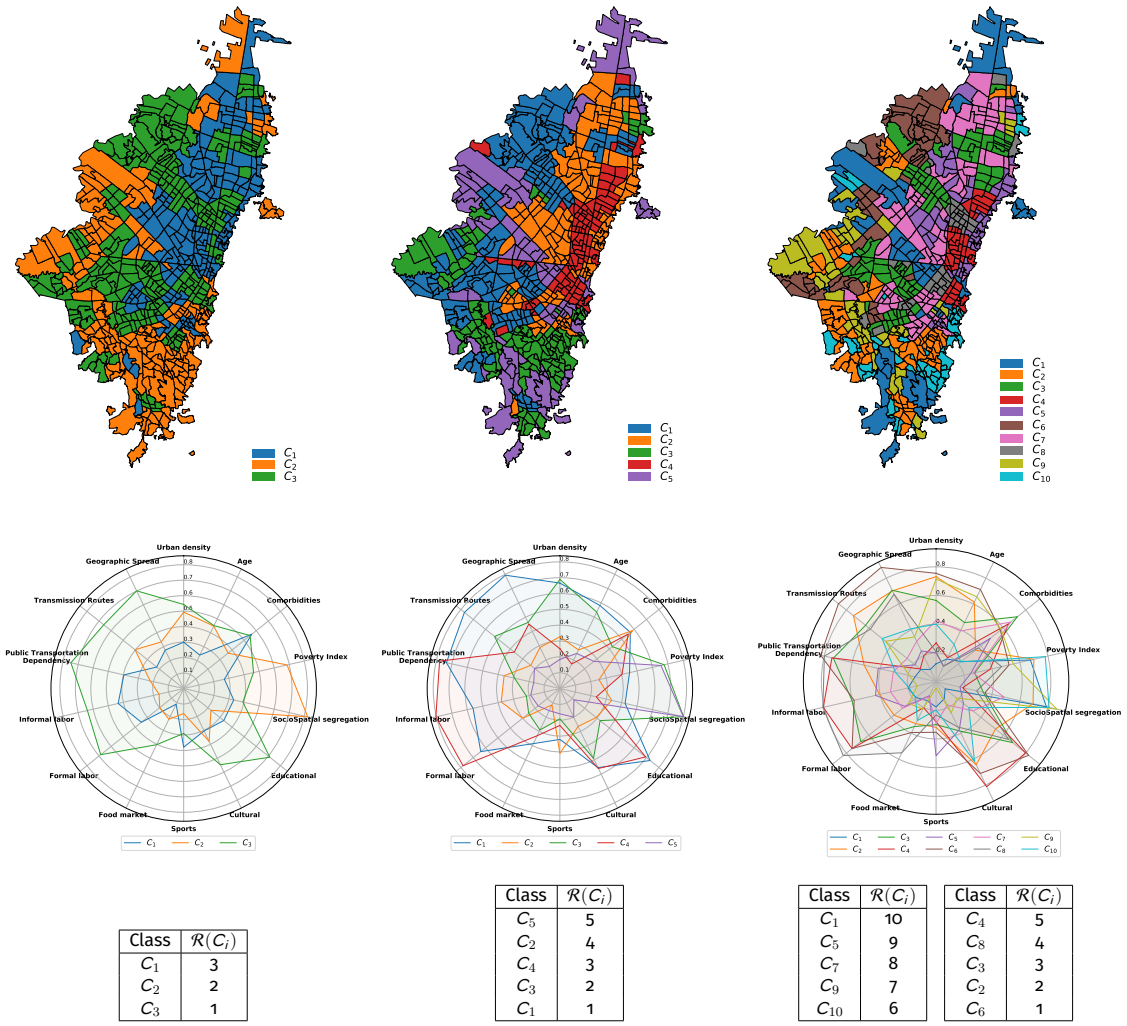

Class	$\mathcal{R}(C_i)$
C_1	3
C_2	2
C_3	1

(A) Vulnerability Ranking I

Class	$\mathcal{R}(C_i)$
C_5	5
C_2	4
C_4	3
C_3	2
C_1	1

(B) Vulnerability Ranking II

Class	$\mathcal{R}(C_i)$
C_1	10
C_5	9
C_7	8
C_9	7
C_{10}	6

Class	$\mathcal{R}(C_i)$
C_4	5
C_8	4
C_3	3
C_2	2
C_6	1

(C) Vulnerability Ranking III

FIGURE 3.3. **Vulnerability Ranking I with $k = 3$ (left panel), Ranking II with $k = 5$ (middle panel), and Ranking III with $k = 10$ (right panel).** For each Vulnerability Ranking: clusters generated using the k-means method (top), its corresponding centroid values for each vulnerable factor (middle), and the unique rank generated using the Borda's count method (bottom). (The class identifier $1, \ldots, k$ for the clusters of the vulnerability indices with different k partitions ($k = 3$ left, $k = 5$ medium, $k = 10$ right) does not be the same between models (i.e., the class identifier variate from index to index).).

Figure 3.4 shows the final three vulnerability index constructed with UVA. In index I, the results show high vulnerable urban sectors in the southwest part of the city. On the other hand, index II shows how some urban sectors change from medium to low or high-vulnerability, with respect the index I. Further, index III presents an interesting scenario where the spatial correlation between urban sectors is not remarkable getting an unbiased vulnerability index for COVID-19.

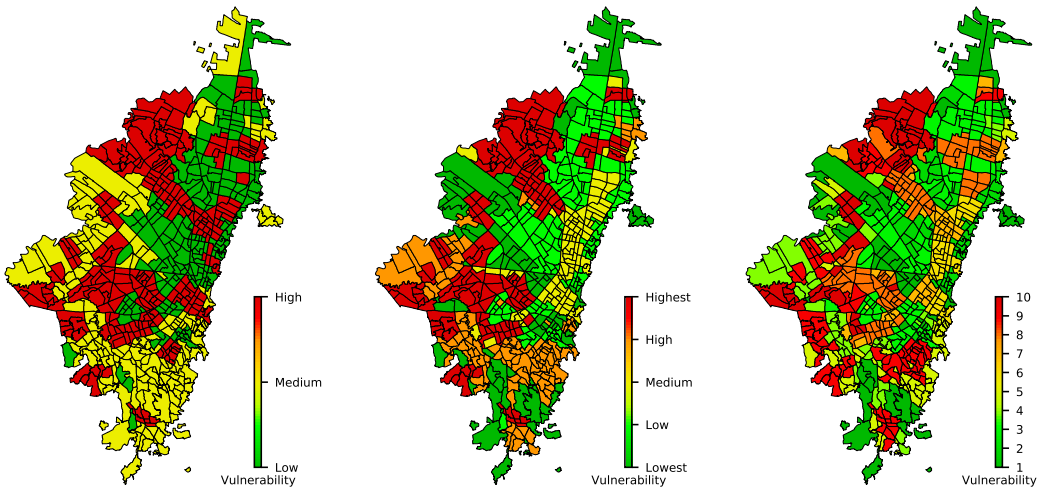

(A) Vulnerability index I (B) Vulnerability index II (C) Vulnerability index III

FIGURE 3.4. **Vulnerability indices generated using Urban Vulnerability Assessment (UVA) for the current COVID-19 pandemic in Bogotá.** Vulnerability index I has 3 levels from low to high (a); Vulnerability index II has 5 levels from lowest to highest (b); and Vulnerability index III has 10 levels from 1 to 10 (c).

Although the intention is not to predict the risk of infection for an urban sector, some similarities between vulnerability indices proposed and the current concentration of COVID-19 cases confirmed in Bogotá [79] can be observed (Figure 3.5). The results show how vulnerable areas found with UVA overlap with urban areas with more COVID-19 cases. This indicates that the UVA framework proposed could be used to recommend actions for before, during, and after a pandemic that is, to planning and coordination efforts through leadership and coordination across sectors, to assess if the risk of a pandemic could increase in specific geographic areas.

3.4 Summary

An Urban Vulnerability Assessment (UVA) for pandemic surveillance is proposed. It is based on a set of 14 vulnerability factors found in the literature. The UVA output defines a composite measure of community-level vulnerability and its spatial distribution, identifying and ranking potentially higher vulnerability areas. The UVA is framed in the current COVID-19 pandemic in Bogotá, the largest and the most crowded city in Colombia. UVA creates not only one, but a set of vulnerability indices (i.e., low-high, lowest-highest, and 1–10) to pandemic surveillance.

The results suggest a connection between high-vulnerability levels and increased impact and spread of the disease at different geographic levels. Therefore, upon thorough evaluation, UVA could become a relevant tool in the development of policies and

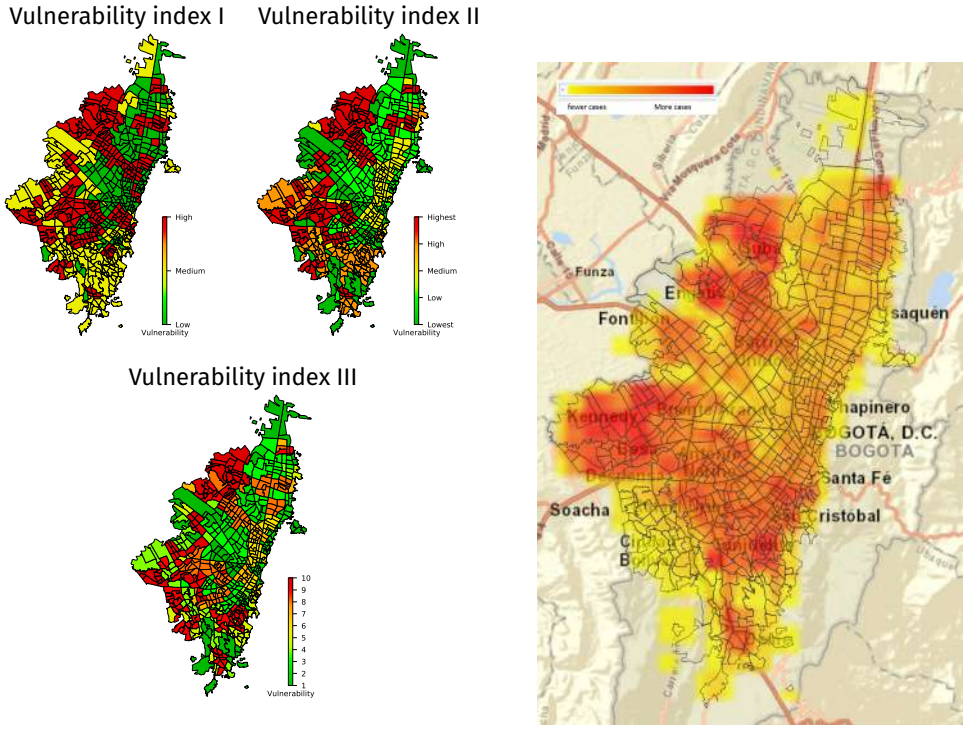

(A) Vulnerability indices proposed in UVA (B) Confirmed COVID-19 cases in Bogotá

FIGURE 3.5. **Comparison between the vulnerability indices proposed in this study (a) and the real COVID-19 cases confirmed in Bogotá (b).** The colored boxes show the concentrations of the cases in 1000 meters on December 30, 2020, in Bogotá, where the red color indicates more confirmed COVID-19 cases and fewer cases are in yellow.

programs aimed at reducing disaster risk (DRR) at different city scales (i.e., addressing urban vulnerability at national, regional, and provincial scales), in diverse scenarios of resource scarcity (i.e., short and long-term actions), and for different audiences (i.e., the citizens, policy-makers, international organizations).

The next chapter introduces a comprehensive risk-based emergency management framework that could be used by decision-makers to determine how best to manage medical resources. The framework uses the vulnerability assessed with UVA to quantify the risk over the spatial units under study.

CHAPTER 4

Risk-based Resource Allocation for pandemic

This chapter establishes a comprehensive risk-based emergency management framework that could be used by decision-makers to determine how best to manage medical resources, as well as suggest patient allocation among hospitals and alternative healthcare facilities. A set of risk indices are proposed by modeling the randomness and uncertainty of allocating resources in a pandemic. The city understudy is modeled as a Euclidean complex network, where depending on the neighborhood influence of allocating a resource in a demand point (i.e., informing citizens, limit social contact, allocate a new hospital) different network configurations are proposed. Finally, a multi-objective risk-based resource allocation (MoRRA) framework is proposed to optimize the allocation of resources in pandemics. The applicability of the framework is shown by the identification of high-risk areas where to prioritize the resource allocation during the current COVID-19 pandemic in Bogotá, Colombia.

4.1 Introduction

Policy attention has focused on the need to identify emerging outbreaks that might lead Pandemics, and to expand investment to build preparedness and health capacity [60]. In the preparedness pandemic, effective allocation of limited health resources (i.e., budget for antivirals and preventive vaccinations, Intensive Care Unit (ICU), ventilators, non-Intensive Care Unit (non-ICU), doctors) plays a critical role in order to reduce the number of cases, hospitalization, and deaths. Despite the great advances in the prevention and treatment of infectious diseases, the world is unaware to respond to a pandemic or any similarly global public-health emergency [83, 65].

In most countries, health care systems operate at or above maximally designed capacity. Many hospitals just do not have sufficient pre-existing resources to respond to

surge capacity in an outbreak [8]. Unlike with natural disasters, where the greatest need for resources often occurs early in the time course, pandemic resource requirements will build over months. Outbreaks that become pandemics generally do not take hold in multiple locations at exactly the same time, they are geographically and temporally patchy [57].

Many government agencies and health planners are responsible for overseeing and monitoring future outbreaks. However, they can't monitor everything all of the time, they have to decide how best to allocate their scarce resources across a broad range of risk exposures. This is called "risk-based resource allocation." [31]. Different types of government agencies face risk-based resource allocation decisions: agricultural land and water resources [94, 125, 62], system design in a Distributed Environment [129, 88], terrorism [124, 89, 90], and Natural Hazards (i.e., tornados, hurricanes, earthquakes) [120, 132, 77]. In the Risk-based resource allocation for pandemic response, a demand point has one (or more) associated risk (i.e., geographic spread, overall poverty, medical preconditions), and the objective is to choose the amount to be invested in several interventions such that the overall risk exposed by the demand points is minimized according to budget constraints and health benefits. Due to the randomness and uncertainty of conditions, not only one but a set of risks may adversely affect the allocation of resources in the geographical space. Then, the objectives (one objective for each risk that a demand point may be exposed) must be optimized simultaneously [128, 113], but there exists a trade-off among objectives, i.e., an improvement gained for one objective is only achieved by making concessions to another objective.

This chapter aims to describe and illustrate a Multi-objective Risk-based Resource Allocation framework (MoRRA) that could be used by decision-makers to determine how best to manage medical resources, as well as suggest patient allocation among hospitals and alternative healthcare facilities. In MoRRA, different definitions of risk-based resource allocation are given depending on the geographical space and its neighborhood configuration. This study is carried out during the COVID-19 in Bogotá, Colombia where identify geographic areas with high-risk factors are identified to prioritize resources to control the outbreak and to generate recommendations for future outbreaks.

The remainder of this chapter is organized as follows. In the next section, the background knowledge, the risk-based resource allocation (RRA) problem, and the formulation of the multi-objective RRA (MoRRA) are given. In Section 4.3, the experimental setup for MoRRA is described and the numerical results of a case study (the current COVID-19 Pandemic in Bogotá, Colombia) are presented. Finally, conclusions and potential future developments are discussed in the last section.

4.2 Risk-based Resource Allocation

Following the risk-based resource allocation methodology presented in Section 1.1, the proposed framework involves three main stages. The first stage is the identification and definition of the risk. The second stage is the estimation of the level of risk posed in a demand point. Once the risk has been defined and measured, an optimal strategy is proposed to minimize the risk exposure.

Risk definition

Following the definition presented in chapter 1.1. Risk is then defined as the expected damages due to a particular hazard for a given area and reference period. Based on mathematical calculations, the risk of the spatial unit i can be determined as a product of hazard (H) and vulnerability (V) [25].

$$R(i) = H(i) \times V(i) \tag{4.1}$$

Risk measuring

Hazard assessment

The hazard assessment describes the identification of what hazards can be expected and how they might change in the short and medium-term as a result of environmental phenomena or processes [50]. First of all, all of the potential hazards are identified. Then the areas that could be affected by the hazard are marked, this is called Hazard Mapping. The magnitude, intensity, and frequency of the hazards are determined.

Vulnerability assessment

Vulnerability Assessment describes the degree to which socioeconomic systems and physical assets in geographic areas are either susceptible or resilient to the impact of a disaster (i.e., pandemic). Several models have been proposed to establish vulnerable urban areas over the infectious disease domain, i.e., vector-borne diseases [42], Dengue [17], malaria [53, 41], Ebola [73], and COVID-19 [69, 86].

Risk strategy

Urban space

Let $\mathcal{S}$ be the geographical space under study (i.e. state, country, or city) defined in terms of a finite set of P smaller spatial units (i.e. countries, census tracts, or zip codes); that is $\mathcal{S} = \{1, 2, \ldots, P\}$. Here the spatial units are located in some position of the 2D

Euclidean complex network $G = (\mathcal{S}, E)$ [117], and the edges E are connection between two nodes given the spatial relation $meet$.

Definition 4.2.1. The spatial relation $meet(i, j)$ occurs when i has at least one point in common with j in the boundary, but their interiors do not intersect [26].

Risk-based Resource Allocation Problem (RRA)

Let Λ be the risk values associated for each spatial unit in $\mathcal{S}$; that is $\Lambda = \{(\lambda_1, \lambda_2, \cdots, \lambda_P) | \lambda_i \in \mathbb{R}^+\}$, the **Risk-based Resource Allocation Problem** looks for the optimal way to allocate the resources R to each demand point (spatial unit) i such that the overall risk over V is minimized. Here, the cost incurred $f_{\Lambda,i}(r_i)$ by allocating the resource r_i at the i-th activity depends on the neighborhood influence of allocating a resource in i (i.e., informing citizens, limit social contact, allocate a new hospital), see equation 4.2.

$$f_{\Lambda,i}(r_i) = \lambda_i(1 - r_i) + \sum_{k \in N(i)} \lambda_k(1 - \alpha_{i,k} r_i) \tag{4.2}$$

where r_i is the impact factor to allocate a resource to the i-th demand point ($0 \leq r_i \leq 1$), $N(i)$ is the neighborhood of i-th demand point, and $\alpha_{i,k}$ is the influence factor in k when a resource is allocated in i ($0 \leq \alpha_{i,k} \leq 1$).

Then, the objective function f_Λ is is calculated among the vertex (spatial units) $\mathcal{S}$.

$$\textbf{min } f_\Lambda(G, R) = \sum_{i=1}^{|\mathcal{S}|} f_{\Lambda,i}(r_i) \tag{4.3}$$

$$\textbf{subject to } \sum_{i=1}^{|R|} r_i \leq T \qquad 0 \leq r_i \leq 1 \tag{4.4}$$

where T (allocation percentage) is the total of spatial units where a resource should be allocated (i.e., $T = 10\%$ means that only 10% of the total space units will receive the resource). Here, depending on the network configuration, three configurations in RRA are proposed (Figure 4.1).

Definition 4.2.2. The **RRA-I** configuration happens when there are not neighborhood influence ($\forall i \in \mathcal{S}, N(i) = \varnothing$). So, the cost incurred $f_{\Lambda,i}(r_i)$ is defined as.

$$f_{\Lambda,i}(r_i) = \lambda_i(1 - r_i) \tag{4.5}$$

Definition 4.2.3. The **RRA-II** configuration happens when there are neighborhood influence at same scale ($\alpha_{i,k} = \alpha$). So, the cost incurred $f_{\Lambda,i}(r_i)$ is defined as.

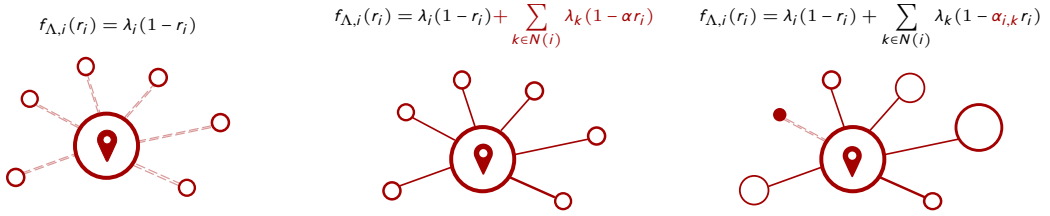

(A) RRA-I (B) RRA-II (C) RRA-III

FIGURE 4.1. **Different configurations of the Risk-based Resource Allocation problem (RRA).** Here, the cost incurred $f_{\Lambda,i}(r_i)$ by allocate the resource r_i at the i-th activity depends on the neighborhood influence. Without neighbor influence (RRA-I) (left), with neighbor influence at same scale (RRA-II) (middle), and with neighbor influence at different scale (RRA-III) (right).

$$f_{\Lambda,i}(r_i) = \lambda_i(1 - r_i) + \sum_{k \in N(i)} \lambda_k(1 - \alpha r_i) \tag{4.6}$$

Definition 4.2.4. The **RRA-III** configuration happens when there is neighborhood influence at a different scale. So, the cost incurred $f_{\Lambda,i}(r_i)$ is defined as.

$$f_{\Lambda,i}(r_i) = \lambda_i(1 - r_i) + \sum_{k \in N(i)} \lambda_k(1 - \alpha_{i,k} r_i) \tag{4.7}$$

Using the adjacency matrix A of G, where the $\alpha_{i,k}$ are the the weight of the edge $w(i,k)$, the objective function can be evaluated in terms of A, see Appendix B.

$$\textbf{min } f_\Lambda(A, R) = \left\| \left(\chi\left(A + I\right) - diag(R)(A + I)\right) \Lambda^T \right\|_1 \tag{4.8}$$

$$\textbf{subject to} \quad \begin{aligned} &\|R\|_1 \leq T \\ &0 \leq r_i \leq 1 \end{aligned} \tag{4.9}$$

where χ is the Indicator function that determines when a value of A is different to 0, I is the identity matrix, $diag$ is the function that diagonalizes the vector of resources R, and Λ are the risks associated with the demand points.

Multi-objective RRA (MoRRA)

Due to the randomness and uncertainty of conditions (environmental, operational), RRA also brings many risks that may adversely affect the allocation of resources in the geographical space. Therefore, it is necessary to introduce a comprehensive set of risk indices by modeling the randomness and uncertainty of the RRA problems. Then, **Multi-objective Risk-based Resource Allocation** aims to optimal way to allocate R to each demand point (spatial unit) i, in a set of M risk indices; that is $\hat{\Lambda} = \{\Lambda_1, \ldots, \Lambda_M\}$.

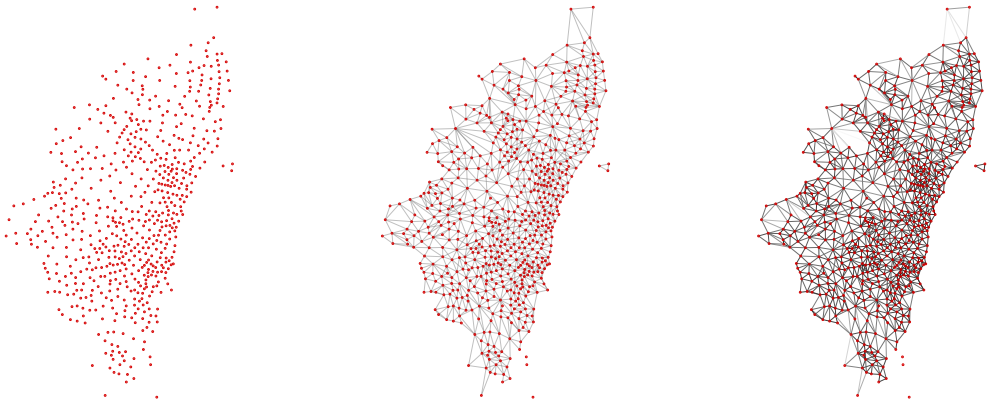

(A) RRA-I (B) RRA-II (C) RRA-III

FIGURE 4.2. **Complex network representation of Bogotá in the three RRA configurations.** RRA-I(left), RRA-II (middle), and RRA-III (right).

$$\begin{aligned} &\textbf{min } f_{\hat{\Lambda}}(G,R) = (f_{\Lambda_1}(G,R),\ldots,f_{\Lambda_M}(G,R))^T \\ &\textbf{subject to } R \in \Omega \end{aligned} \tag{4.10}$$

4.3 Resource allocation for COVID-19 in Bogotá

Urban Space definition

The complex network for Bogotá (using the Urban sector as the spatial unit) in the different RRA configurations is built (Figure 4.2). For RRA-II, the α value is set to 0.5, which means that influence in the neighborhood when a resource is allocated is half. For RRA-III, the α_{ik} values are set depending on the distance between vertex; that is less distance more influence. The α_{ik} are normalized over the range 0 (less influence) and 0.5 (more influence).

Risk definition in COVID-19

Pandemic hazard Disasters (i.e., the COVID-19 pandemic) rarely exist, because they are social, arising from a combination of hazard and vulnerability, with vulnerability as the causative factor. This kind of disaster occurs at multiple levels simultaneously, with responses to a hazard exposing as many vulnerability problems as the original hazard. The failure to heed to the pandemic plans alongside the lack of health-care accessible to everyone meant that the hazard could not be addressed effectively and vulnerability fundamentals were revealed [51].

Then, based on mathematical calculations, we assume that the hazard (the new coronavirus) is constant for all spatial units; that is $\forall i \in \mathcal{S}, H(i) = 1$.

Pandemic vulnerability

Three domains are proposed on [86] to describe the vulnerability for the COVID-19 in Bogotá, Colombia. Those domains are: (i) Where and how a person lives (life), (ii) Where and how a person works (work), and (iii) Where and how a person moves around (movement). Table 3.2 (previous chapter) shows the domains proposed, the vulnerability factors associated with them, and the dataset used to calculate the values for each factor.

Then, based on mathematical calculations, a spatial unit i has associated three vulnerable factors: life, work, and movement; that is $\forall i \in \mathcal{S}, V(i) = \{V_{life}(i), V_{work}(i), V_{movement}(i)\}$.

Risk assessment in COVID-19

Taking the hazard as constant $H(i) = 1$, the Vulnerability Assessment is the only part to worry about. In the previous chapter, a framework for Urban Vulnerability Assessment (UVA) is introduced. UVA condenses a set of vulnerability factors (Table 3.2) into a vulnerability index that allowed us to establish and rank potentially vulnerable urban areas in Bogotá. To build the vulnerability index for the three vulnerable domains (life, work, and movement), the following steps are applied:

1. The raw data for each factor is normalized across all spatial units over the range 0 (best) to 1 (worst). The normalization is already calculated in [86].
2. Synthesize the normalized information of all spatial units into k partitions which groups spatial units with similar vulnerability profiles. Here, $k = 10$ is chosen to generate 10 ranges of vulnerabilities (from 0.5 to 0.95, with step of 0.1).
3. The clusters' centroids of each group are used to sort the vulnerability factors in descending order. This sort is interpreted as vulnerability ranking which is used for the analysis.
4. Then, to aggregate the L ranks (one for each vulnerable factor, then for life $L = 5$, work $L = 6$, movement $L = 3$) in a unique vulnerability ranking the Borda's method is used.
5. The unique vulnerability ranking is then transformed into a vulnerability index, where a higher rank indicates higher vulnerability.

The output of this process is the three vulnerability indices (one for each domain).

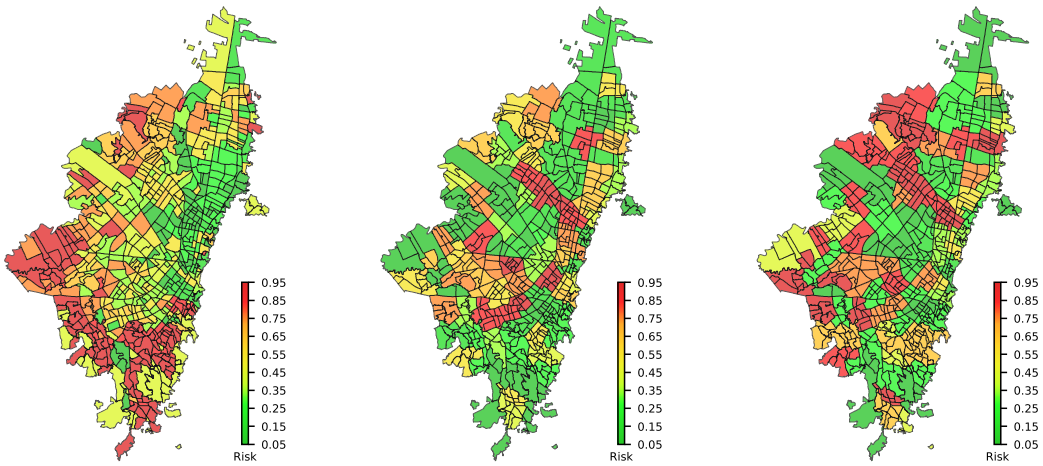

(A) Life risk (B) Work risk (C) Movement risk

FIGURE 4.3. **Risk indices generated for the current COVID-19 pandemic in Bogota.**

Finally, to quantify the risk, this study follows the risk definition presented in 4.1. As $H(i)$ is assumed as constant, the risk indices are associated with the vulnerability indices, i.e., $Life(i) = V_{life}(i)$, $Work(i) = V_{work}(i)$, and $Movement(i) = V_{movement}(i)$ are the life risk, work risk and movement risk, respectively; for the spatial unit i. Figure 4.3 shows the final three risk indices.

Risk strategy in COVID-19

Experimental Setup

To solve the formulated multi-objective risk-based resource allocation problem, a comparison with different multi-objective algorithms (MOEA/D [130], NSGA-III [21], RVEA [11], and ARMOEA [114]) are made on different configurations (i.e., RRA-I, RRA-II, RRA-III) and different allocation percentages (i.e., $T = 10\%$, $T = 25\%$, $T = 50\%$). Here, the impact factor r_i is assumed to 0.5, which means that allocates a resource in the spatial unit i would reduce the risk in half. Values of T and r_i are estimated based on the observations made in the experiments.

Compared Algorithms: The following four state-of-the-art algorithms for multi-objective functions are considered as peer algorithms.

- MOEA/D [130]: It is representative of the decomposition-based method, the basic idea of MOEA/D is to decompose a MOP into several single-objective optimization subproblems through aggregation functions and simultaneously optimizes them.

- NSGA-III [21]: It is based on decomposition with Pareto-adaptive weight vectors. This approach automatically adjusts the weight vectors by the geometrical characteristics of the Pareto front.
- RVEA [11]: It is a scalarization approach, and termed angle penalized distance approach that dynamically adjusts the distribution of the reference vectors to balance convergence and diversity of the solutions in the PFs.
- ARMOEA [114]: It uses an enhanced inverted generational distance indicator, in which an adaptation method adjusts a set of reference points based on the indicator contributions of candidate solutions.

Performance Metrics: To evaluate the performance of different algorithms for the RRA problems, each algorithm is run for the same number of generations, and the resulting solutions (known as Pareto front approximations), are compared using functions that measure two qualities: (i) solution accuracy, i.e., to determine how similar the solution is to the true Pareto front and (ii) solution diversity, i.e., to evaluate how well distributed are the points in the solution. Two of the most used metrics called Δ_p [101] and Coverage over Pareto Front (CPF) [115] are selected to compare the accuracy and the diversity of the solutions found by the different algorithms.

Parameter Setting: Here, the general parameter settings for the experiments are presented, and afterward, the specific parameter settings for each algorithm in comparison are given.

1. Genetic operators: The widely used genetic operators, i.e., simulated binary crossover (SBX) [19] and the polynomial mutation (PM) [20] are employed to create the offspring population.
   - SBX: A real-coded crossover operator whose search power is better than binary-coded GAs with the single point crossover. SBX is defined in terms of the probability of creating an arbitrary child solution from a given pair of parent solutions.
   - PM: A real-coded mutation operator whose uses a polynomial probability distribution to perturb the solution in a parent's vicinity. The probability distribution in both left and right of a variable value is adjusted so that no value outside the specified range [a, b] is created.

   For the SBX, the distribution index is set to $\eta_c = 30$ and the crossover probability $p_c = 1.0$ is used in all algorithms; for PM the distribution index and the mutation probability are set to $\eta_m = 20$ and $p_m = 1/n$, respectively.
2. Population size: The algorithms chosen for the comparison use a predefined set of reference points to ensure diversity in obtained solutions. The experiments uses

the Das and Dennis's [15] systematic approach that places points on a *normalized hyper-plane* (M – 1)- dimensional unit simplex. If p divisions are considered along each objective, the total number of reference points (H) in an M-objective problem is given by:

$$H = \binom{M + p + 1}{p}$$

How the population size is dependent on H, using $p = 12$, as recommended in [130, 21, 11, 114], and $M = 3$ (objective functions - life, work and movement risks), the population size is set to 91 individuals.

3. Termination Condition: Every algorithm stops when the number of function evaluations reaches the maximum number. For all configurations and allocation percentages, the maximal number of generations is set to 10000, as recommended in [130, 21, 11, 114].

4. Specific Parameter Settings in Each Algorithm: For MOEA/D, the weights vectors are calculated using the penalty-based boundary intersection (PBI), the neighborhood size T is set to 20, and the penalty parameter θ in PBI is set to 5, as recommended in [130]. For RVEA, the parameter controlling the rate of change of penalty (α) and the frequency of employing reference vector adaptation (fr) are to 2 and 0.1, respectively, as recommended in [11].

Results

The methodology of MoRRA (Data preprocessing; MATLAB code; PFs; and visualization) is available in a Github repository, see Appendix A.

Pareto front

The statistical results of the Δ_p and CPF metrics values obtained by the four algorithms for the different configurations and allocation percentages over 20 independent runs are summarized in Table 4.1, where the best results are highlighted. The Wilcoxon rank-sum test is adopted to compare the results obtained by the four compared algorithms at a significance level of 0.05 (here, the MOEA/D algorithm is taken as the reference's algorithm). Symbol '$+$' indicates that MOEA/D is significantly outperformed by the compared algorithm according to a Wilcoxon rank-sum test, while '$-$' means that the compared algorithm is significantly outperformed by MOEA/D. Finally, '$\approx$' means that there is no statistically significant difference between the results obtained by MOEA/D and the compared algorithm. It can be seen that MOEA/D shows the best overall performance among the four compared algorithms over the Δ_p metric in the experiments, while RVEA shows the best overall performance over the CPF metric in experiments. The results obtained by RVEA (good performance on Δ_p and CPF) in the different con-

TABLE 4.1. **Statistics Δ_p and CPF metric values of the Pareto-optimal solutions found by the four compared algorithms for the different RRA configurations and amount allocations.** The numbers in parentheses are the standard deviations.

Metric	Problem	Amount	MOEA/D	NSGAIII	RVEA	ARMOEA
Δ_p	RRA-I	10%	4.887e+2 (8.97e-1)	4.902e+2 (6.71e-1) –	**4.883e+2 (6.70e-1)** ≈	4.890e+2 (6.77e-1) ≈
		25%	**4.437e+2 (1.25e+0)**	4.467e+2 (1.24e+0) –	4.440e+2 (1.19e+0) ≈	4.443e+2 (1.26e+0) ≈
		50%	**3.751e+2 (1.73e+0)**	3.788e+2 (1.42e+0) –	3.759e+2 (1.84e+0) ≈	3.768e+2 (1.39e+0) –
	RRA-II	10%	3.564e+3 (3.32e+0)	3.572e+3 (2.19e+0) –	**3.562e+3 (4.88e+0)** +	3.568e+3 (3.37e+0) –
		25%	**3.384e+3 (4.36e+0)**	3.399e+3 (4.99e+0) –	3.388e+3 (8.34e+0) ≈	3.393e+3 (6.69e+0) –
		50%	**3.113e+3 (4.39e+0)**	3.129e+3 (5.26e+0) –	3.116e+3 (8.36e+0) ≈	3.121e+3 (6.79e+0) –
	RRA-III	10%	**3.588e+3 (2.92e+0)**	3.594e+3 (2.40e+0) –	3.588e+3 (3.13e+0) ≈	3.592e+3 (2.61e+0) –
		25%	**3.441e+3 (4.08e+0)**	3.452e+3 (3.18e+0) –	3.442e+3 (5.50e+0) ≈	3.446e+3 (4.12e+0) –
		50%	**3.211e+3 (4.73e+0)**	3.226e+3 (4.81e+0) –	3.215e+3 (6.46e+0) –	3.219e+3 (6.00e+0) –
CPF	RRA-I	10%	7.920e-2 (3.67e-2)	1.193e-1 (2.99e-2) +	**2.160e-1 (5.06e-2)** +	1.028e-1 (3.08e-2) ≈
		25%	6.570e-2 (3.96e-2)	1.264e-1 (2.79e-2) +	**2.044e-1 (7.11e-2)** +	1.009e-1 (4.06e-2) +
		50%	6.940e-2 (3.18e-2)	1.267e-1 (2.49e-2) +	**1.938e-1 (5.20e-2)** +	1.112e-1 (3.77e-2) +
	RRA-II	10%	3.287e-2 (3.09e-2)	1.188e-1 (5.11e-2) +	**1.803e-1 (4.85e-2)** +	1.316e-1 (5.39e-2) ≈
		25%	2.397e-2 (2.01e-2)	1.244e-1 (6.34e-2) +	**2.210e-1 (8.94e-2)** +	1.213e-1 (4.84e-2) +
		50%	3.584e-2 (2.11e-2)	1.248e-1 (4.90e-2) +	**2.432e-1 (8.10e-2)** +	1.413e-1 (9.87e-2) +
	RRA-III	10%	3.908e-2 (2.94e-2)	1.217e-1 (3.99e-2) +	**2.273e-1 (6.45e-2)** +	1.244e-1 (5.90e-2) +
		25%	4.659e-2 (3.33e-2)	1.053e-1 (3.28e-2) +	**2.001e-1 (5.78e-2)** +	1.088e-1 (3.70e-2) +
		50%	2.554e-2 (1.99e-2)	1.272e-1 (2.89e-2) +	**2.205e-1 (6.75e-2)** +	1.080e-1 (3.68e-2) +

+: MOEA/D shows significantly worse performance in the comparison.
–: MOEA/D shows significantly better performance in the comparison.
≈: There is no significant difference between the compared results.

figurations and allocation percentages will be used in the rest of this section for the following results.

The range of the *non-dominated* solutions found with RVEA are shown in Figure 4.4. The *Pareto front* behavior shows promising convergence performance as well as a good distribution on problems with different configurations and allocation percentages.

Decision making

To visualize the solution in the Bogotá network map, a pseudo-weight vector approach proposed in [18] is used. This method calculates the normalized distance to the best solution regarding each objective.

First, one solution is selected with equal pseudo-weights ($w_{life} = 1/3$, $w_{work} = 1/3$, $w_{movement} = 1/3$) for each different RRA configurations and allocation percentages equal to $\%10$ (Figure 4.5). The results shows an interesting scenario where the spatial correlation between urban sectors is not remarkable getting an unbiased risk-based resource allocation for COVID-19.

Further, Figure 4.6 shows the solutions found with MoRRA in the real COVID-19 cases confirmed in Bogotá. This results indicate that the MoRRA framework proposed could be used to recommend actions for before, during, and after a pandemic that is, to planning and coordination efforts through leadership and coordination across sectors, to assess if the risk of a pandemic could increase in specific geographic areas.

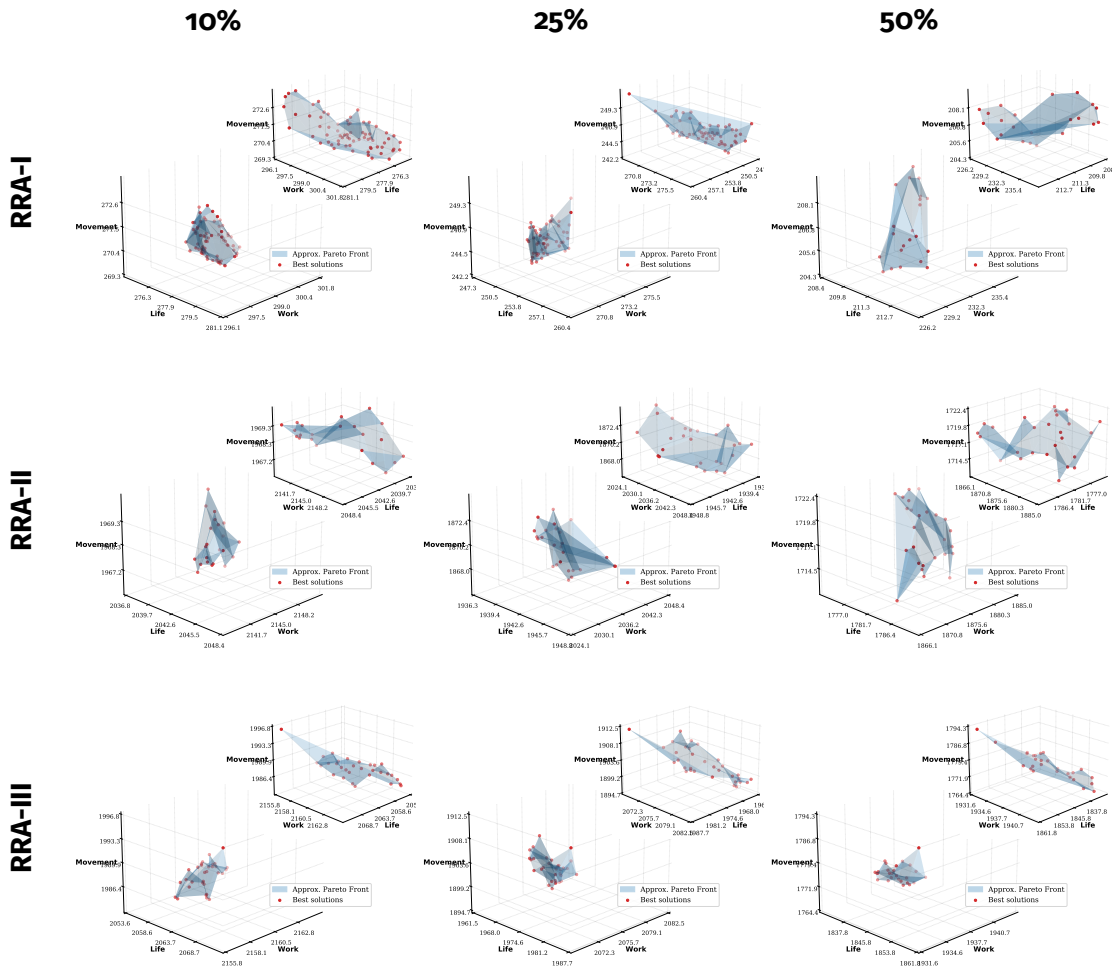

FIGURE 4.4. **The approximate Pareto optimal solutions obtained by RVEA on problems with different configurations (RRA-I, RRA-II, RRA-III) and allocation percentages (10%, 25%, 50%).**

4.4 Summary

A Multi-objective Risk-based Resource Allocation (MoRRA) framework for Pandemic Preparedness is proposed. MoRRA could be used to build evidence for planning, modeling, and epidemiological studies to better inform the public, policymakers, and international organizations and funders as to where and how to improve surveillance, response efforts, and delivery of resources. The proposed MoRRA is tested in the current COVID-19 Pandemic in Bogotá city, the largest and crowded city in Colombia. MoRRA creates not only one, but a set of risk indices (i.e., life, work, movement) and uses it to apply the risk-based resource allocation.

Although the risk factors involved in the framework are structural, the proposed approach is flexible, does not require expert support or knowledge, and allows policymakers, and international organizations to prioritize resource allocation in short and

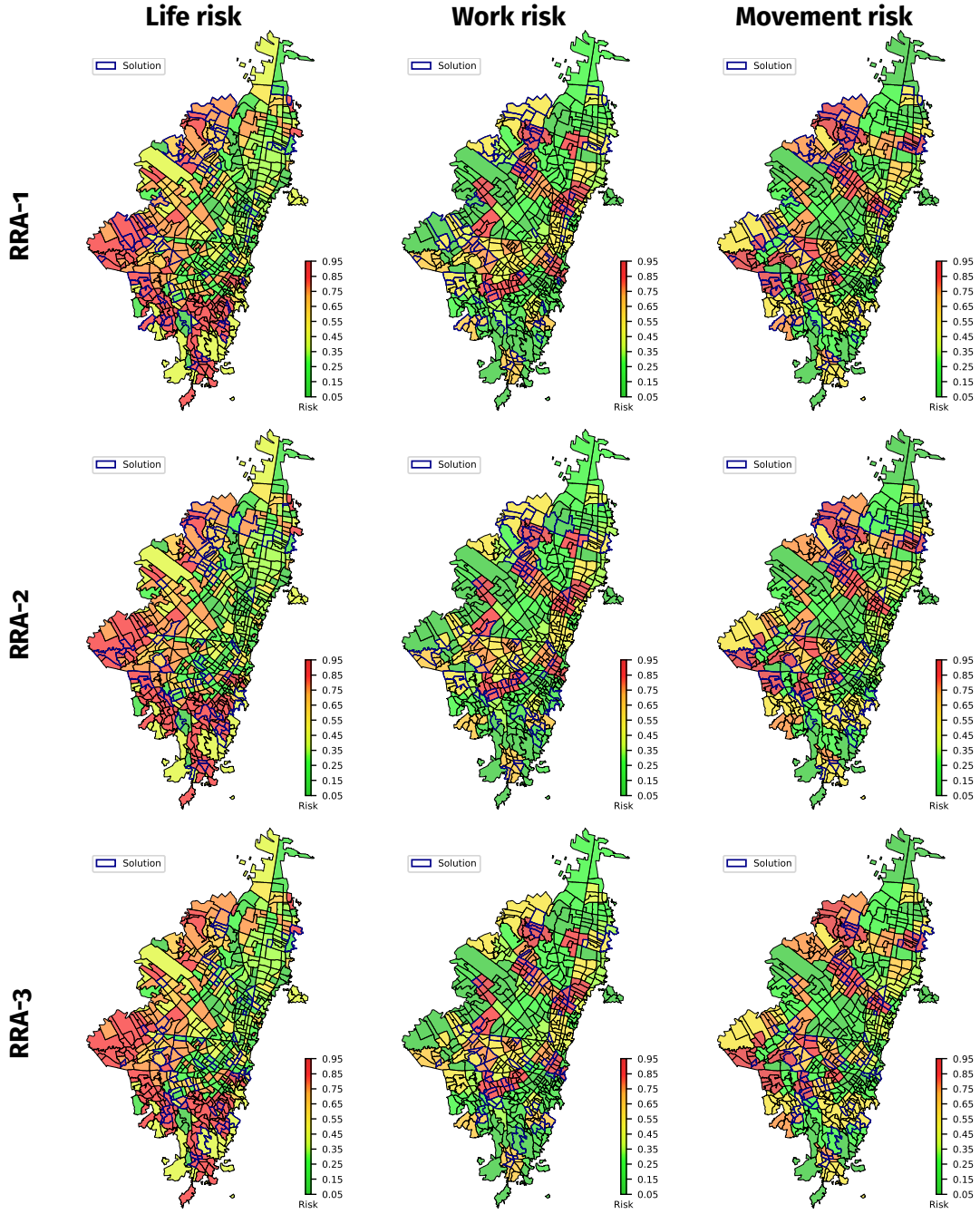

FIGURE 4.5. **Solution visualized in Bogotá with different configurations of RRA and 10% of allocation percentage using equal pseudo-weights ($w_{life} = 1/3, w_{work} = 1/3, w_{movement} = 1/3$).**

long-term actions for affected populations in a city. For instance, using the solutions with more weight in the movement risk a short-actions (i.e, staying home, limit close contact, avoid crowds, limit non-essential travel) can be taken to reduce the risk in the city. Further, using the solutions with more weight in the life risk, it is possible to advance in long-term territorial reorganization plans (i.e., reduce socio-spatial segregation, decent housing, bio-secure protocols for high-density facilities) as the results indicate for the COVID-19 in the urban area of Bogotá.

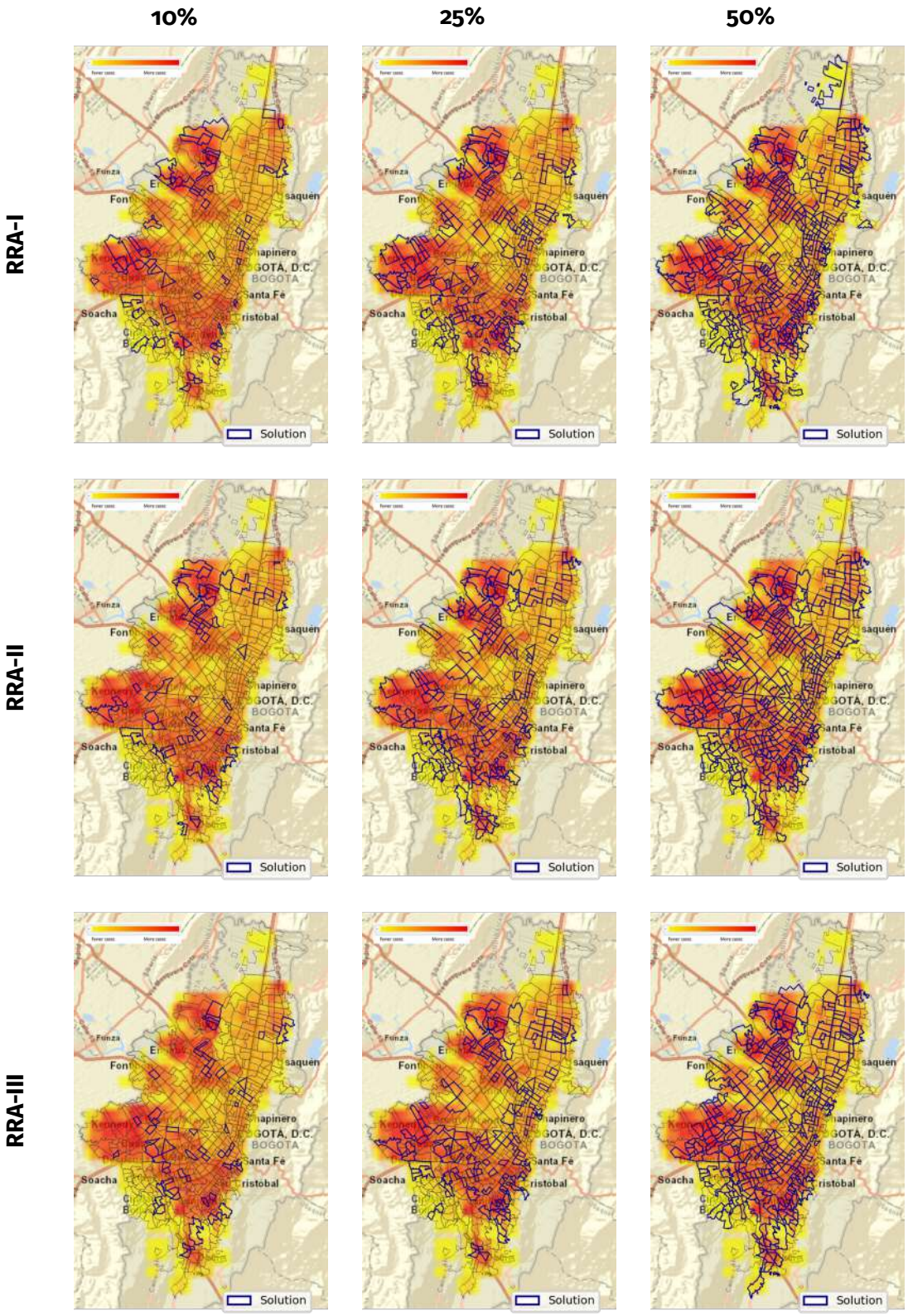

FIGURE 4.6. **Solutions found with MoRRA over the real COVID-19 cases confirmed in Bogotá.** The colored boxes show the concentrations of the cases in 1000 meters on December 30, 2020, in Bogotá, where the red color indicates more confirmed COVID-19 cases and fewer cases are in yellow.

Conclusions and Future work

Conclusions

Resource allocation in a pandemic presents an intractable problem because unlike natural disasters, where the greatest need for resources often occurs early in the course of time, pandemic resource requirements generally take hold in multiple locations at the same time (i.e., they are geographically and temporally patchy). Different frameworks have tried to solve the problem of resource allocation in a pandemic, but all of them have issues that must be resolved before one can even begin to attempt a solution: the role of medicine as a monopolistic profession, the ethical status of the goods and services, and role social values.

Since the problem of resource allocation in a pandemic can be done using a risk management perspective, it is possible to integrate different risk-based models to find a solution for it. This thesis addresses the problem of Risk-based Resource Allocation suitable to be used for supporting decision-making in the formulation of management and response policies during a Pandemic.

The main contribution is a framework that could become a relevant tool in the development of policies and programs aimed at reducing disaster risk (DRR) at different city scales (i.e., addressing urban vulnerability at national, regional, and provincial scales), in diverse scenarios of resource scarcity (i.e., short and long-term actions), and for different audiences (i.e., the citizens, policy-makers, international organizations). Especially:

- An agent-based model, called INFEKTA, for simulating the transmission of infectious diseases, not only the COVID-19, under social distancing policies is presented. INFEKTA combines the transmission dynamic of a specific disease with demographic information of geopolitical regions of the real town or city under study. Results were published and indicate that INFEKTA may be a valuable asset for researchers and public health decision-makers for exploring future scenarios

when applying different social distancing policy rules and controlling the expansion of an infectious disease.

- An Urban Vulnerability Assessment framework, called UVA, is introduced. UVA investigates various vulnerability factors related to pandemics (severity of infection and transmissibility) to assess the vulnerability in urban areas. A vulnerability index is constructed by the aggregation of multiple vulnerability factors computed on each urban area (i.e., urban density, poverty index, informal labor, transmission routes). The results suggest a connection between high-vulnerability levels and increased impact and spread of the disease at different geographic levels.

- A comprehensive risk-based emergency management framework, called MoRRA is presented. MoRRA could be used by decision-makers to determine how best to manage medical resources, as well as suggest patient allocation among hospitals and alternative healthcare facilities. A set of risk indices are proposed by modeling the randomness and uncertainty of allocating resources in a pandemic. The results indicate that the MoRRA framework could be used to recommend actions for before, during, and after a pandemic that is, to planning and coordination efforts through leadership and coordination across sectors, to assess if the risk of a pandemic could increase in specific geographic areas.

- Finally, the transmission disease model (INFEKTA), the vulnerability assessment framework (UVA), and the comprehensive risk-based emergency management framework (MoRRA) were tested in the current COVID-19 pandemic in Bogotá, the capital of Colombia.

Future work

The contributions and results obtained in this thesis open several perspectives for further research in this important field.

One direction is in the INFEKTA model. Here, the work will concentrate on studying the transmission of COVID-19 in Bogotá by considering different scenarios of social distancing rules and by using more realistic information about: i) Relation between personal information and propagation rates of the COVID-19, ii) Places and routes, iii) Population size, and iv) Age and Medical preconditions.

On the other hand, in the UVA framework, it would be possible to calculate the index at the neighborhood level. Furthermore, the relative importance of the assessment criteria to assign weights to construct the vulnerability index is an issue to be addressed in future research. Also, data used in this study are 1–4 years old and might not have captured vulnerability well in urban sectors in which rapid changes have occurred up to the present day.

Finally, in the MoRRA framework, the work will concentrate on the executing and learning step in the risk-based resource allocation strategy. To conduct risk-management activities, such as inspections, getting feedback on what is working and what is not, and learning from that feedback could improve the decision-making process. Furthermore, scaling to other cities, or even at the country level is a possibility that can be covered in the future.

Bibliography

[1] Rajib Acharya and Akash Porwal. A vulnerability index for the management of and response to the COVID-19 epidemic in India: an ecological study. *The Lancet Global Health*, 8(9):e1142–e1151, 2020.

[2] Óscar Alfonso. Densidades divergentes y segregación socio-espacial en la Bogotá de hoy: un análisis a partir de un índice de calidad de la densidad. In *VIII Seminario Internacional de Investigación en Urbanismo, Barcelona-Balneário Camboriú, Junio 2016*, 2016.

[3] Ethem Alpaydin. *Introduction to machine learning*. MIT press, 2020.

[4] Nezih Altay and Walter G Green III. OR/MS research in disaster operations management. *European journal of operational research*, 175(1):475–493, 2006.

[5] Gary An, Qi Mi, Joyeeta Dutta-Moscato, and Yoram Vodovotz. Agent-based models in translational systems biology. *WIREs Systems Biology and Medicine*, 1(2):159–171, 2009.

[6] John E Angus. The probability integral transform and related results. *SIAM review*, 36(4):652–654, 1994.

[7] P. G. Balaji and D. Srinivasan. An introduction to multi-agent systems. *Studies in Computational Intelligence*, 310:1–27, 2010.

[8] E Lee Daugherty Biddison, Ruth Faden, Howard S Gwon, Darren P Mareiniss, Alan C Regenberg, Monica Schoch-Spana, Jack Schwartz, and Eric S Toner. Too many patients... a framework to guide statewide allocation of scarce mechanical ventilation during disasters. *Chest*, 155(4):848–854, 2019.

[9] Sheryl L Chang, Nathan Harding, Cameron Zachreson, Oliver M Cliff, and Mikhail Prokopenko. Modelling transmission and control of the COVID-19 pandemic in Australia. *Nature communications*, 11(1):1–13, 2020.

[10] Mark IC Chen, Vernon JM Lee, Ian Barr, Cui Lin, Rachelle Goh, Caroline Lee, Baldev Singh, Jessie Tan, Wei-Yen Lim, Alex R Cook, et al. Risk factors for pandemic (H1N1) 2009 virus seroconversion among hospital staff, Singapore. *Emerging infectious diseases*, 16(10):1554, 2010.

[11] Ran Cheng, Yaochu Jin, Markus Olhofer, and Bernhard Sendhoff. A reference vector guided evolutionary algorithm for many-objective optimization. *IEEE Transactions on Evolutionary Computation*, 20(5):773–791, 2016.

[12] Matteo Chinazzi, Jessica T Davis, Marco Ajelli, Corrado Gioannini, Maria Litvinova, Stefano Merler, Ana Pastore y Piontti, Kunpeng Mu, Luca Rossi, Kaiyuan Sun, et al. The effect of travel restrictions on the spread of the 2019 novel coronavirus (COVID-19) outbreak. *Science*, 368(6489):395–400, 2020.

[13] Philip Cooley, Bruce Y Lee, Shawn Brown, James Cajka, Bernadette Chasteen, Laxminarayana Ganapathi, James H Stark, William D Wheaton, Diane K Wagener, and Donald S Burke. Protecting health care workers: a pandemic simulation based on Allegheny County. *Influenza and other respiratory viruses*, 4(2):61–72, 2010.

[14] Damon P Coppola. *Introduction to international disaster management*. Elsevier, 2006.

[15] Indraneel Das and John E Dennis. Normal-boundary intersection: A new method for generating the Pareto surface in nonlinear multicriteria optimization problems. *SIAM journal on optimization*, 8(3):631–657, 1998.

[16] Michael Day. Covid-19: four fifths of cases are asymptomatic, China figures indicate, 2020.

[17] Maria Cristina de Mattos Almeida, Waleska Teixeira Caiaffa, Renato Martins Assunçao, and Fernando Augusto Proietti. Spatial vulnerability to dengue in a Brazilian urban area during a 7-year surveillance. *Journal of Urban Health*, 84(3):334–345, 2007.

[18] Kalyanmoy Deb. Multi-objective optimisation using evolutionary algorithms: an introduction. In *Multi-objective evolutionary optimisation for product design and manufacturing*, pages 3–34. Springer, 2011.

[19] Kalyanmoy Deb, Ram Bhushan Agrawal, et al. Simulated binary crossover for continuous search space. *Complex systems*, 9(2):115–148, 1995.

[20] Kalyanmoy Deb and Mayank Goyal. A combined genetic adaptive search (GeneAS) for engineering design. *Computer Science and informatics*, 26:30–45, 1996.

[21] Kalyanmoy Deb and Himanshu Jain. An evolutionary many-objective optimization algorithm using reference-point-based nondominated sorting approach, part I: solving problems with box constraints. *IEEE transactions on evolutionary computation*, 18(4):577–601, 2013.

[22] Departamento Administrativo Nacional de Estadística. COLOMBIA - Censo Nacional de Población y Vivienda - CNPV - 2018, 2018.

[23] Departamento Administrativo Nacional de Estadística. Pobreza multidimensional en Colombia, 2018.

[24] Departamento Administrativo Nacional de Estadística. Índice de vulnerabilidad por manzana con el uso de variables demográficas y comorbilidades, 2020.

[25] UN DHA. Internationally agreed glossary of basic terms related to disaster management. *UN DHA (United Nations Department of Humanitarian Affairs), Geneva*, 1992.

[26] Max Egenhofer. A mathematical framework for the definition of topological relations. In *Proc. the fourth international symposium on spatial data handing*, pages 803–813, 1990.

[27] Peter Emerson. The original Borda count and partial voting. *Social Choice and Welfare*, 40(2):353–358, 2013.

[28] Wayne TA Enanoria, Fengchen Liu, Jennifer Zipprich, Kathleen Harriman, Sarah Ackley, Seth Blumberg, Lee Worden, and Travis C Porco. The effect of contact investigations and public health interventions in the control and prevention of measles transmission: a simulation study. *PloS one*, 11(12):e0167160, 2016.

[29] Joshua M Epstein, Ramesh Pankajakshan, and Ross A Hammond. Combining computational fluid dynamics and agent-based modeling: A new approach to evacuation planning. *PloS one*, 6(5):e20139, 2011.

[30] María Elena Escobar-Ospina and Jonatan Gómez. *"Artificial Life and Therapeutic Vaccines Against Cancers that Originate in Viruses"*, pages 149–305. Springer International Publishing, Cham, 2019.

[31] Diana Farrell, Biniam Gebre, Claudia Hudspeth, and Andrew Sellgren. Risk-based resource allocation. *McKinsey Center for Government*, 2013.

[32] Neil Ferguson, Daniel Laydon, Gemma Nedjati Gilani, Natsuko Imai, Kylie Ainslie, Marc Baguelin, Sangeeta Bhatia, Adhiratha Boonyasiri, ZULMA Cucunuba Perez, Gina Cuomo-Dannenburg, et al. Report 9: Impact of non-pharmaceutical interventions (NPIs) to reduce COVID19 mortality and healthcare demand. 2020.

[33] Neil M Ferguson, Derek AT Cummings, Simon Cauchemez, Christophe Fraser, Steven Riley, Aronrag Meeyai, Sopon Iamsirithaworn, and Donald S Burke. Strategies for containing an emerging influenza pandemic in Southeast Asia. *Nature*, 437(7056):209–214, 2005.

[34] Barry E Flanagan, Edward W Gregory, Elaine J Hallisey, Janet L Heitgerd, and Brian Lewis. A social vulnerability index for disaster management. *Journal of homeland security and emergency management*, 8(1), 2011.

[35] Seth Flaxman, Swapnil Mishra, Axel Gandy, H Juliette T Unwin, Helen Coupland, Thomas A Mellan, Harrison Zhu, Tresnia Berah, Jeffrey W Eaton, Pablo NP Guzman, et al. Estimating the number of infections and the impact of non-pharmaceutical interventions on covid-19 in european countries: technical description update. *arXiv preprint arXiv:2004.11342*, 2020.

[36] Sandro Galea, Matthew Riddle, and George A Kaplan. Causal thinking and complex system approaches in epidemiology. *International journal of epidemiology*, 39(1):97–106, 2010.

[37] Geoffrey P Garnett, Simon Cousens, Timothy B Hallett, Richard Steketee, and Neff Walker. Mathematical models in the evaluation of health programmes. *The Lancet*, 378(9790):515–525, 2011.

[38] Edward Goldstein and Marc Lipsitch. Temporal rise in the proportion of younger adults and older adolescents among coronavirus disease (covid-19) cases following the introduction of physical distancing measures, germany, march to april 2020. *Eurosurveillance*, 25(17):2000596, 2020.

[39] Jonatan Gomez, Jeisson Prieto, Elizabeth Leon, and Arles Rodríguez. INFEKTA—An agent-based model for transmission of infectious diseases: The COVID-19 case in Bogotá, Colombia. *PloS one*, 16(2):e0245787, 2021.

[40] Joel Grus. *Data science from scratch: first principles with python*. O'Reilly Media, 2019.

[41] Michael Hagenlocher and Marcia C Castro. Mapping malaria risk and vulnerability in the United Republic of Tanzania: a spatial explicit model. *Population health metrics*, 13(1):1–14, 2015.

[42] Michael Hagenlocher, Stefan Kienberger, Stefan Lang, and Thomas Blaschke. Implications of spatial scales and reporting units for the spatial modelling of vulnerability to vector-borne diseases. *GI_Forum*, 2014:197, 2014.

[43] M Elizabeth Halloran, Ira M Longini, Azhar Nizam, and Yang Yang. Containing bioterrorist smallpox. *Science*, 298(5597):1428–1432, 2002.

[44] International Labour Organisation. COVID-19 crisis and the informal economy: immediate responses and policy challenges. 2020.

[45] Mark Jit and Marc Brisson. Modelling the epidemiology of infectious diseases for decision analysis. *Pharmacoeconomics*, 29(5):371–386, 2011.

[46] Rachel E Jordan, Peymane Adab, and KK Cheng. Covid-19: risk factors for severe disease and death, 2020.

[47] Sung-mok Jung, Andrei R Akhmetzhanov, Katsuma Hayashi, Natalie M Linton, Yichi Yang, Baoyin Yuan, Tetsuro Kobayashi, Ryo Kinoshita, and Hiroshi Nishiura. Real-time estimation of the risk of death from novel coronavirus (COVID-19) infection: inference using exported cases. *Journal of clinical medicine*, 9(2):523, 2020.

[48] Naoki Katoh and Toshihide Ibaraki. Resource allocation problems. In *Handbook of combinatorial optimization*, pages 905–1006. Springer, 1998.

[49] Rebecca Katz. Use of revised International Health Regulations during influenza A (H1N1) epidemic, 2009. *Emerging infectious diseases*, 15(8):1165, 2009.

[50] Ilan Kelman. Lost for words amongst disaster risk science vocabulary? *International Journal of Disaster Risk Science*, 9(3):281–291, 2018.

[51] Ilan Kelman. COVID-19: what is the disaster? *Social Anthropology*, 2020.

[52] William Ogilvy Kermack and Anderson G McKendrick. A contribution to the mathematical theory of epidemics. *Proceedings of the royal society of london. Series A, Containing papers of a mathematical and physical character*, 115(772):700–721, 1927.

[53] Stefan Kienberger and Michael Hagenlocher. Spatial-explicit modeling of social vulnerability to malaria in East Africa. *International journal of health geographics*, 13(1):1–16, 2014.

[54] István Z Kiss, Joel C Miller, Péter L Simon, et al. Mathematics of epidemics on networks. *Cham: Springer*, 598, 2017.

[55] Mikko Kivelä, Raj Kumar Pan, Kimmo Kaski, János Kertész, Jari Saramäki, and Márton Karsai. Multiscale analysis of spreading in a large communication network. *Journal of Statistical Mechanics: Theory and Experiment*, 2012(03):P03005, 2012.

[56] Maciej Komosinski and Andrew Adamatzky. *Artificial Life Models in Software*. Springer Publishing Company, Incorporated, 2nd edition, 2014.

[57] Melik Koyuncu and Rizvan Erol. Optimal resource allocation model to mitigate the impact of pandemic influenza: a case study for Turkey. *Journal of medical systems*, 34(1):61–70, 2010.

[58] James Ladyman, James Lambert, and Karoline Wiesner. What is a complex system? *European Journal for Philosophy of Science*, 3(1):33–67, 2013.

[59] Pat Langley. Systematic and nonsystematic search strategies. In *Artificial Intelligence Planning Systems*, pages 145–152. Elsevier, 1992.

[60] Joshua Lederberg, Margaret A Hamburg, Mark S Smolinski, et al. *Microbial threats to health: emergence, detection, and response*. National Academies Press, 2003.

[61] J Lessler, WJ Edmunds, ME Halloran, TD Hollingsworth, and AL Lloyd. Seven challenges for model-driven data collection in experimental and observational studies. *Epidemics*, 10:78–82, 2015.

[62] Mo Li, Ping Guo, Vijay P Singh, and Gaiqiang Yang. An uncertainty-based framework for agricultural water-land resources allocation and risk evaluation. *Agricultural Water Management*, 177:10–23, 2016.

[63] Jingzhou Liu, Jinshan Wu, and ZR Yang. The spread of infectious disease on complex networks with household-structure. *Physica A: Statistical Mechanics and its Applications*, 341:273–280, 2004.

[64] Douglas A Luke and Katherine A Stamatakis. Systems science methods in public health: dynamics, networks, and agents. *Annual review of public health*, 33:357–376, 2012.

[65] Nita Madhav, Ben Oppenheim, Mark Gallivan, Prime Mulembakani, Edward Rubin, and Nathan Wolfe. Pandemics: risks, impacts, and mitigation. In *Disease Control Priorities: Improving Health and Reducing Poverty. 3rd edition*. The International Bank for Reconstruction and Development/The World Bank, 2017.

[66] David McLoughlin. A framework for integrated emergency management. *Public administration review*, 45:165–172, 1985.

[67] Emanuela Merelli, Matteo Rucco, Peter Sloot, and Luca Tesei. Topological characterization of complex systems: Using persistent entropy. *Entropy*, 17(10):6872–6892, 2015.

[68] Robert A Meyers. *Encyclopedia of Complexity and Systems Science*. Springer, New York, NY, 2009.

[69] Swasti Vardhan Mishra, Amiya Gayen, and Sk Mafizul Haque. COVID-19 and urban vulnerability in India. *Habitat international*, 103:102230, 2020.

[70] Melanie Mitchell and Mark Newman. *Complex Systems Theory and Evolution*. Oxford University Press, 2005.

[71] D Mitlin. Dealing with COVID-19 in the towns and cities of the global South. *IIED Blogs*, 27, 2020.

[72] Clyde L Monma, Alexander Schrijver, Michael J Todd, and Victor K Wei. Convex resource allocation problems on directed acyclic graphs: duality, complexity, special cases, and extensions. *Mathematics of Operations Research*, 15(4):736–748, 1990.

[73] Melinda Moore, Bill Gelfeld, and Christopher Paul Adeyemi Okunogbe. Identifying future disease hot spots: infectious disease vulnerability index. *Rand health quarterly*, 6(3), 2017.

[74] Stephen S Morse. Factors in the emergence of infectious diseases. In *Plagues and politics*, pages 8–26. Springer, 2001.

[75] Joël Mossong, Niel Hens, Mark Jit, Philippe Beutels, Kari Auranen, Rafael Mikolajczyk, Marco Massari, Stefania Salmaso, Gianpaolo Scalia Tomba, Jacco Wallinga, et al. Social contacts and mixing patterns relevant to the spread of infectious diseases. *PLoS medicine*, 5(3), 2008.

[76] Enrique Mu and Milagros Pereyra-Rojas. *Practical decision making: an introduction to the Analytic Hierarchy Process (AHP) using super decisions V2*. Springer, 2016.

[77] Colleen Murphy and Paolo Gardoni. Determining public policy and resource allocation priorities for mitigating natural hazards: A capabilities-based approach. *Science and Engineering Ethics*, 13(4):489–504, 2007.

[78] Megan Murray. Determinants of cluster distribution in the molecular epidemiology of tuberculosis. *Proceedings of the National Academy of Sciences*, 99(3):1538–1543, 2002.

[79] Observatorio de Salud de Bogotá. Casos confirmados de COVID-19 en Bogotá, 2020.

[80] Ben Oppenheim, Mark Gallivan, Nita K Madhav, Naor Brown, Volodymyr Serhiyenko, Nathan D Wolfe, and Patrick Ayscue. Assessing global preparedness for the next pandemic: development and application of an Epidemic Preparedness Index. *BMJ global health*, 4(1):e001157, 2019.

[81] Pan American Health Organization. Leadership during a pandemic: What your municipality can do, 2009.

[82] World Health Organization. *International health regulations (2005).* World Health Organization, 2008.

[83] World Health Organization. Report of the review committee on the functioning of the international health regulations (2005) in relation to pandemic (H1N1) 2009. *Sixty-fourth World Health Assembly: World Health Organization*, pages 49–50, 2011.

[84] Jeisson Prieto and Jonatan Gomez. Multi-objective risk-based resource allocation for urban pandemic preparedness: The covid-19 case in bogotá, colombia. *medRxiv*, 2021.

[85] Jeisson Prieto, Jonatan Gomez, and Elizabeth Leon. Multi-objective evolutionary algorithm for DNA codeword design. In *Proceedings of the Genetic and Evolutionary Computation Conference*, pages 604–611, 2019.

[86] Jeisson Prieto, Rafael Malagón, Jonatan Gomez, and Elizabeth León. Urban vulnerability assessment for pandemic surveillance—the covid-19 case in bogotá, colombia. *Sustainability*, 13(6):3402, 2021.

[87] United Nations Development Programme. Covid-19 pandemic humanity needs leadership and solidarity to defeat the coronavirus, 2020.

[88] Yuming Qiu, Ping Ge, and Solomon C Yim. Risk-based resource allocation for collaborative system design in a distributed environment. *Journal of Mechanical Design*, 130(6), 2008.

[89] Luca Quadrifoglio. A bottom-up risk-based resource allocation methodology to counter terrorism. *International journal of society systems science*, 1(1):4–25, 2008.

[90] J Ray, PT Boggs, DM Gay, MN Lemaster, and ME Ehlen. Risk-based decision making for staggered bioterrorist attacks: Resource allocation and risk reduction in "reload" scenarios. *Sandia Report, SAND2009-6008*, 2009.

[91] Alireza Rezaei and Sadra Tahsili. Urban vulnerability assessment using AHP. *Advances in Civil Engineering*, 2018, 2018.

[92] Arles Rodríguez, Jonatan Gómez, and Ada Diaconescu. Towards failure-resistant mobile distributed systems inspired by swarm intelligence and trophallaxis. In *Artificial Life Conference Proceedings 13*, pages 448–455. MIT Press, 2015.

[93] Arles Rodríguez, Jonatan Gómez, and Ada Diaconescu. Exploring complex networks with failure-prone agents. In *Mexican International Conference on Artificial Intelligence*, pages 81–98. Springer, 2016.

[94] Carlos Romero. Risk programming for agricultural resource allocation: A multidimensional risk approach. *Annals of Operations Research*, 94(1-4):57–68, 2000.

[95] Stuart Russell and Peter Norvig. *Artificial intelligence a modern approach*. Prentice-Hall, New Jersey, third edition, 2010.

[96] Jorge Salas and Víctor Yepes. Urban vulnerability assessment: Advances from the strategic planning outlook. *Journal of Cleaner Production*, 179:544–558, 2018.

[97] Jorge Salas and Víctor Yepes. VisualUVAM: A decision support system addressing the curse of dimensionality for the multi-scale assessment of urban vulnerability in Spain. *Sustainability*, 11(8):2191, 2019.

[98] Marcel Salathé and James H Jones. Dynamics and control of diseases in networks with community structure. *PLoS computational biology*, 6(4), 2010.

[99] Hiroki Sayama. *Introduction to the modeling and analysis of complex systems*. Binghamton University, SUNY, 2015.

[100] SF Schultz. *Disaster relief logistics: benefits of and impediments to horizontal cooperation between humanitarian organizations*. PhD thesis, Tese. Technischen Universität Berlin, 2008.

[101] Oliver Schutze, Xavier Esquivel, Adriana Lara, and Carlos A Coello Coello. Using the averaged Hausdorff distance as a performance measure in evolutionary multiobjective optimization. *IEEE Transactions on Evolutionary Computation*, 16(4):504–522, 2012.

[102] David W Scott. *Multivariate density estimation: theory, practice, and visualization*. John Wiley & Sons, 2015.

[103] Secretaría Distrital de Movilidad. *Observatorio de Movilidad Bogotá D.C. 2017*, 2017.

[104] Secretaría Distrital de Planeación. *Monografías de las localidades Bogotá D.C. 2011*, 2011.

[105] Secretaría Distrital de Planeación. Información, cartografía y estadística, 2016.

[106] Secretaría Distrital de Planeación. *Monografías de las localidades Bogotá D.C. 2017*, 2017.

[107] Secretaría Distrital de Planeación. Población UPZ Bogotá, 2017.

[108] Secretaría Distrital de Planeación. *Determinantes de la distribución espacial de la informalidad laboral en Bogotá*, 2018.

[109] Clara Stegehuis, Remco Van Der Hofstad, and Johan SH Van Leeuwaarden. Epidemic spreading on complex networks with community structures. *Scientific reports*, 6(1):1–7, 2016.

[110] Subgerencia Técnica y Servicios Bogotá D.C. Trazados Troncales de TRANSMILENIO, 2019.

[111] Jennifer A Summers, Nick Wilson, Michael G Baker, and G Dennis Shanks. Mortality risk factors for pandemic influenza on New Zealand troop ship, 1918. *Emerging infectious diseases*, 16(12):1931, 2010.

[112] HJ Sun and ZY Gao. Dynamical behaviors of epidemics on scale-free networks with community structure. *Physica A: Statistical Mechanics and its Applications*, 381:491–496, 2007.

[113] Li Sun, Gail W DePuy, and Gerald W Evans. Multi-objective optimization models for patient allocation during a pandemic influenza outbreak. *Computers & Operations Research*, 51:350–359, 2014.

[114] Ye Tian, Ran Cheng, Xingyi Zhang, Fan Cheng, and Yaochu Jin. An indicator-based multiobjective evolutionary algorithm with reference point adaptation for better versatility. *IEEE Transactions on Evolutionary Computation*, 22(4):609–622, 2017.

[115] Ye Tian, Ran Cheng, Xingyi Zhang, Miqing Li, and Yaochu Jin. Diversity Assessment of Multi-Objective Evolutionary Algorithms: Performance Metric and Benchmark Problems [Research Frontier]. *IEEE Computational Intelligence Magazine*, 14(3):61–74, 2019.

[116] UN Habitat. *UN-habitat COVID-19 response plan*, 2020.

[117] Remco Van Der Hofstad. *Random Graphs and Complex Networks Vol. I.*, volume I. Cambridge Series in Statistical and Probabilistic Mathematics, 2017.

[118] Durk-Jouke van der Zee. Approaches for simulation model simplification. In *2017 Winter Simulation Conference (WSC)*, pages 4197–4208. IEEE, 2017.

[119] Esther van Kleef, Julie V Robotham, Mark Jit, Sarah R Deeny, and William J Edmunds. Modelling the transmission of healthcare associated infections: a systematic review. *BMC infectious diseases*, 13(1):294, 2013.

[120] Pantea Vaziri, Rachel A Davidson, Linda K Nozick, and Mahmood Hosseini. Resource allocation for regional earthquake risk mitigation: a case study of Tehran, Iran. *Natural hazards*, 53(3):527–546, 2010.

[121] Robert Verity, Lucy C Okell, Ilaria Dorigatti, Peter Winskill, Charles Whittaker, Natsuko Imai, Gina Cuomo-Dannenburg, Hayley Thompson, Patrick GT Walker, Han Fu, et al. Estimates of the severity of coronavirus disease 2019: a model-based analysis. *The Lancet infectious diseases*, 20(6):669–677, 2020.

[122] Rozann Whitaker. Criticisms of the Analytic Hierarchy Process: Why they often make no sense. *Mathematical and Computer Modelling*, 46(7-8):948–961, 2007.

[123] Lander Willem, Frederik Verelst, Joke Bilcke, Niel Hens, and Philippe Beutels. Lessons from a decade of individual-based models for infectious disease transmission: a systematic review (2006-2015). *BMC infectious diseases*, 17(1):612, 2017.

[124] Henry H Willis. Guiding resource allocations based on terrorism risk. *Risk Analysis: An International Journal*, 27(3):597–606, 2007.

[125] Jerome M Wolgin. Resource allocation and risk: A case study of smallholder agriculture in Kenya. *American Journal of Agricultural Economics*, 57(4):622–630, 1975.

[126] World Health Organization. *Coronavirus disease 2019 (COVID-19): Situation report, 40*, 2020.

[127] Bo Xu, Moritz UG Kraemer, and Data Curation Group. Open access epidemiological data from the COVID-19 outbreak. *The Lancet. Infectious Diseases*, 2020.

[128] Zhenyu Yan and Yacov Y Haimes. Risk-based multiobjective resource allocation in hierarchical systems with multiple decisionmakers. Part I: Theory and methodology. *Systems Engineering*, 14(1):1–16, 2011.

[129] Sree Rama Kumar Yeddanapudi, Yuan Li, James D McCalley, Ali A Chowdhury, and Ward T Jewell. Risk-based allocation of distribution system maintenance resources. *IEEE Transactions on Power Systems*, 23(2):287–295, 2008.

[130] Qingfu Zhang and Hui Li. MOEA/D: A multiobjective evolutionary algorithm based on decomposition. *IEEE Transactions on evolutionary computation*, 11(6):712–731, 2007.

[131] Wen Zhao, Shikai Yu, Xiangyi Zha, Ning Wang, Qiumei Pang, Tongzeng Li, and Aixin Li. Clinical characteristics and durations of hospitalized patients with COVID-19 in Beijing: a retrospective cohort study. *MedRxiv*, 2020.

[132] Mohammad R Zolfaghari and Elnaz Peyghaleh. Implementation of equity in resource allocation for regional earthquake risk mitigation using two-stage stochastic programming. *Risk analysis*, 35(3):434–458, 2015.

APPENDIX

Appendix A: Supplementary Material

INFEKTA repository. A repository containing the source code of the simulator and a technical report explaining the modeling methodology is available at INFEKTA github.

UVA repository. A repository containing the source code of the vulnerability assessment methodology and a technical report explaining the modeling is available at UVA github.

MoRRA repository. A repository containing the source code of the multi-objective resource allocation problem and a technical report explaining the modeling methodology is available at MoRRA github.

APPENDIX

Appendix B: Matrix Notation of RRA

To derive (4.8) for (4.3), the Euclidean Complex Network G is represented with its adjacency matrix A. Then, I want to demonstrate.

$$\textbf{min } f_\Lambda(G, R) = \textbf{min } f_\Lambda(A, R)$$

when $f_\Lambda(A, R)$ is written as.

$$f_\Lambda(A, R) = \left\|(\chi(A + I) - diag(R)(A + I))\Lambda^T\right\|_1$$

Here, χ is the indicator function that determines when a value of A is different to 0, I is the identity matrix, $diag$ is the function that diagonalize the vector of resources R, and Λ are the risks associated with the demand points.

Expanding $f_\Lambda(A, R)$, we have.

$$f_\Lambda(A, R) = \left\|\left(\begin{bmatrix} 1 & \dots & \hat{\alpha}_{1,p} \\ \vdots & \ddots & \\ \hat{\alpha}_{p,1} & & 1 \end{bmatrix} - \begin{bmatrix} r_1 & \dots & 0 \\ \vdots & \ddots & \\ 0 & & r_p \end{bmatrix} \begin{bmatrix} 1 & \dots & \alpha_{1,p} \\ \vdots & \ddots & \\ \alpha_{p,1} & & 1 \end{bmatrix}\right) \begin{bmatrix} \lambda_1 \\ \vdots \\ \lambda_p \end{bmatrix}\right\|_1$$

where $\alpha_{i,j}$ is 1 where exist an edge between i and j and it is 0 otherwise (indicator function χ). Solving.

$$
\begin{aligned}
f_\Lambda(A,R) &= \left\| \left(\begin{bmatrix} 1 & \dots & \hat{\alpha}_{1,p} \\ \vdots & \ddots & \\ \hat{\alpha}_{p,1} & & 1 \end{bmatrix} - \begin{bmatrix} r_1 & \dots & r_1\alpha_{1,p} \\ \vdots & \ddots & \\ r_p\alpha_{p,1} & & r_p \end{bmatrix} \right) \begin{bmatrix} \lambda_1 \\ \vdots \\ \lambda_p \end{bmatrix} \right\|_1 \\
&= \left\| \begin{bmatrix} 1-r_1 & \dots & \hat{\alpha}_{1,p} - r_1\alpha_{1,p} \\ \vdots & \ddots & \\ \hat{\alpha}_{p,1} - r_p\alpha_{p,1} & & 1-r_p \end{bmatrix} \begin{bmatrix} \lambda_1 \\ \vdots \\ \lambda_p \end{bmatrix} \right\|_1 \\
&= \left\| \begin{bmatrix} \lambda_1(1-r_1) + \dots + \lambda_p(\hat{\alpha}_{1,p} - r_1\alpha_{1,p}) \\ \vdots \\ \lambda_1(\hat{\alpha}_{p,1} - r_p\alpha_{p,1}) + \dots + \lambda_p(1-r_p) \end{bmatrix} \right\|_1
\end{aligned}
$$

Grouping similar terms.

$$
f_\Lambda(A,R) = \left\| \begin{bmatrix} \lambda_1(1-r_1) + \sum_{k\in N(1)} \lambda_k(1-\alpha_{1,k}r_1) \\ \vdots \\ \lambda_p(1-r_p) + \sum_{k\in N(p)} \lambda_k(1-\alpha_{p,k}r_p) \end{bmatrix} \right\|_1
$$

Each term in the column vector can be written as (4.2).

$$
f_\Lambda(A,R) = \left\| \begin{bmatrix} f_{\Lambda,i}(r_i) \\ \vdots \\ f_{\Lambda,p}(r_p) \end{bmatrix} \right\|_1
$$

Applying 1-Norm.

$$
f_\Lambda(A,R) = \sum_{i=1}^{|\mathcal{S}|} f_{\Lambda,i}(r_i)
$$

So, it is sufficient to prove that (4.3) could be written as (4.8) when the graph G is representing by its adjacency matrix A.